Verification of the numerical wave model SWAN in the Petten coastal area

Committee:
Prof. dr. Ir. J.A. Battjes
dr. Ir. L.H. Holthuijsen
Ir. J.H. Andorka Gal

Den Haag,april 1997

J.C.M de Jong

Abstract

Due to the new act on the water defense the Directorate-General of Public Works and Water Management of the Netherlands is required to evaluate the design conditions for the coastal defenses every five years. To do this evaluation a model is needed to translate offshore wave conditions to nearshore design conditions. For such transformations numerical wave models SWAN and HISWA are available. These models take the relevant processes of wave propagation, generation and dissipation into account.

During the storms of January of 1995 a measurement campaign was conducted. From this campaign wave data was obtained to verify the numerical wave models. The wave measurements were taken on a 8.3 km long transect perpendicular to the coastline. Placed 8.3 km offshore there is 1 wave rider buoy to register the incoming waves. Further 2 buoys, 1 pressure transducer and 1 wave staff are used. Three storm situations with waterlevels of 2 m (+ NAP), incoming significant wave heights between 4.5 m and 5.1 m and peak periods between 10.0 s and 14.3 s are used.

These situations are modeled with SWAN and HISWA and wave parameters as well as spectra are compared to the wave parameters and spectra. It shows that the results of the SWAN computations for significant wave height are within 6% accuracy. The results of HISWA computations are with 10 % accuracy. The mean zero crossing periods in SWAN are within 10 % of the observed. Spectra reproduced in SWAN resemble well with the observed spectra.

Table of contents

1 Introduction

1.1 General introduction

Due to the new act on the water defense the Directorate-General of Public Works and Water Management of the Netherlands is required to evaluate the design conditions for the coastal defenses every five years. To do this one has to know the design conditions for each part of the coast, so the National Institute for Coastal & Marine Management / *RIKZ*, which is an institute of the Ministry of Transport, Public Works and Water Management of the Netherlands, has set up the HYDRA-project. HYDRA has three objectives:

1. To translate deep water wave conditions to shallow water wave conditions.
2. To translate wave data from one location to spatial data.
3. To extrapolate normal storm conditions to extreme storm conditions.

A part of HYDRA is the Case Study Petten to which the first two objectives apply. Case Study Petten will be exemplary for the whole Dutch closed coastline. In this study two numerical wave propagation models (SWAN & HISWA) will be validated for this case study with the data obtained from a measurement campaign at Petten conducted in January of 1995. A sensitivity study of the SWAN model will also be carried out.

1.2 Problem

To design coastal defenses properly, it is necessary to predict extreme water level and wave conditions. To obtain these, a statistical evaluation of water levels and wave conditions is needed. In general, it is not convenient to take the measurements, needed for this statistical evaluation, at nearshore locations (near the toe of the dike) because:

1: Measurements near the coast provide data for one specific place only. Therefore, it would be necessary to have a lot of measuring points to obtain data for the entire coast, because nearshore data are not applicable to all positions along the shore-line
2: Managers of sea-dikes will not allow measuring devices or other instruments to be implanted in their dikes.

If the measurements would be taken offshore and transferred to nearshore design conditions, far fewer measuring sites would be needed.

To transfer the offshore wave conditions a (2-dimensional wave) model is needed. In this study two numerical wave propagation models (SWAN & HISWA) developed by Delft University of Technology are used. These models are based on the action balance equation. A brief description of SWAN is given in section 2.2.2 and of HISWA in section 2.2.3. A more extensive description of SWAN is given in Ris et.al. (1996) and of HISWA in Booij et.al. (1995).

To know how the wave models perform it is necessary to know the wave conditions in reality and compare the results from computations with these observations. For this verification the data acquired in an extensive measuring campaign in the storm season of 1994 -1995 were used. The measurements were taken during two different storms in January 1995., [Andorka Gal (1996)].

So offshore wave boundary conditions have to be translated to nearshore wave boundary conditions. The main question in this report is, 'How do SWAN and HISWA perform at the Petten coastal area?'

1.2.1 Problem definition and aim

There are no comparisons between numerical wave models (SWAN & HISWA) and measurements for the Petten coastal area.

So the aim is to apply and verify the numerical wave models SWAN and HISWA at the Petten coastal area with the measurement data acquired in January of 1995.

1.2.2 Problem approach

In this study SWAN & HISWA will be applied to the Petten coastal area and compared with measurements from January 1st, 2nd and 10th of 1995. Situations to be modeled were selected from the data acquired. The times are selected such, that data are present from each day with different shapes of the spectrum measured offshore and data are present for all stations.

From the sounding data and an existing bottom depth schematization, a bottom depth schematization for the sea area around the 'Pettemer Polder' is made. This schematization represents the bottom topography in the numerical computations used for the storm of January 1995.

With these data three computations with SWAN are made to compare results with the measurements. Three other SWAN computations for the same periods are made with boundary conditions acquired from data of permanent offshore measuring stations (Eierlandse Gat and IJmuiden, ELD and YMW). The differences in the results for these two approaches are investigated and presented. For all three cases the results of the SWAN computations are compared to results of HISWA computations for the same situations.

The SWAN and HISWA computations are made with standard model settings for all three cases. For one case in SWAN a sensitivity study to numerics, boundary conditions and physical parametrization is performed.

The numerical computations differ in spatial resolution and in directional resolution.

In the sensitivity study to boundary conditions the following boundary conditions have been changed to see the effect they have nearshore. The water level is increased so higher waves can pass the banks. The peak period of the input spectrum is increased to see the effect of this higher frequency. The windspeed is increased which should result in more wave growth. The incoming wave height is changed to see the effect of offshore waveheight in the model.

In the sensitivity study to physical schematization the following parameters of modeled physical processes are changed. The effects of bottom friction is not taken into account in one computation. The breaker index is set to a lower value. The non-linear triad interaction is turned off in one computation and set to a stronger interaction value in another computation and another wind input formulation is used.

Finally conclusions are drawn and recommendations for further studies are made.

1.3 Outline of this report

Chapter one contains the introduction.

In chapter two a brief description of wind waves and of the numerical wave models SWAN & HISWA are given.

Chapter three gives the origin of the data used in this report. Here the three cases to be modeled are decided upon.

Chapter four describes the way SWAN is used in the Petten coastal area. It describes the cases in which the standard setting of the input parameters and sizes and orientations of the grids are given.

In chapter five the sensitivity study is described.

In chapter six a comparison between the results for SWAN cycle 1 and HISWA is made.

And finally in chapter seven the conclusions and recommendations of this study are given.

2 Wave modeling

2.1 Wind waves

Wind generated waves have irregular periods and wave heights, caused by the irregular nature of wind. Due to this irregular nature the sea surface is continually varying, which means a deterministic approach to describe this surface is not suitable. However it is possible to consider wind waves as a superposition of many sinusoidal waves with random phases, frequencies, amplitudes and directions (linear wave theory). The free surface elevation in one point as a function of time can be described as:

$$\eta(t) = \sum a_i \cos(2\pi f_i t + \alpha_i)$$

with

$\eta(t)$	= the free surface elevation [m]
a_i	= the amplitude of the i^{th} cosine component [m]
f_i	= the frequency of the i^{th} cosine component [Hz]
α_i	= the random phase of the i^{th} cosine component
t	= time [s]

$\eta(t)$ is used to determine the energy density function E(f), which gives the distribution of energy over the frequencies.. E(f) is proportional to a^2. The total energy is the area under the 1-D energy density spectrum or the volume under the 2-D spectrum (figure 2-1).

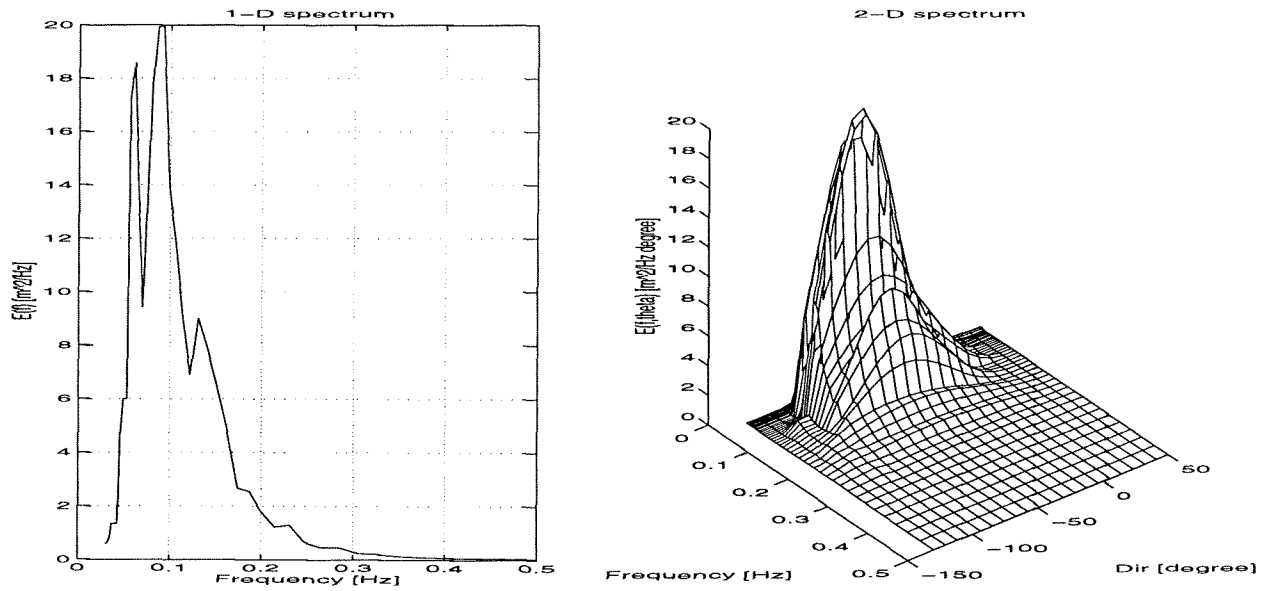

figure 2-1 1-D and 2-D spectra (2-D spectrum presented in a quasi 3-D fashion)

Spectral wave parameters are expressed as moments of the energy density function E(f):

$$m_n = \int_0^\infty f^n E(f) df \quad n = 0,1,2$$

with

m_n = the n^{th} moment of the spectrum

With these moments some wave parameters are described:

Characteristic wave height:

Hm_0	$= 4\sqrt{(m_0)}$	significant wave height $=H_s$.

Characteristic periods:

Tm_{01}	$= m_0/m_1$	average period
Tm_{02}	$=\sqrt{(m_0/m_2)}$	average period

Another characteristic period:

T_p	$= 1/f_m$	the peak-period this is the period were the spectrum has its maximum energy density.

2.2 The wave models

2.2.1 General

The development of wave prediction methods started in order to get reliable predictions of wave conditions for the landing of the allied forces in the second world war. A major improvement in wave prediction during late '50's was the introduction of the energy density spectrum from electrotechnics and acoustics. It is possible to describe a wave field that varies in space and time with the two dimensional energy density spectrum (figure 2-1).

The change of energy density per unit time in a coordinate system that moves with the group velocity in the direction of the wave component is equal to the sum of energy growth and decay per unit time. The sum of energy growth and decay in time is called the source function. The source function can be divided in three separate terms. The first is a term representing energy input by the wind field. The second term represents energy dissipation (like bottom dissipation and wave breaking). The third term represents nonlinear wave-wave interactions.

$$\frac{dE}{dt} = S_{in} + S_{ds} + S_{nl}$$

2.2.2 SWAN

The model SWAN (which is an acronym for Simulation of Waves Nearshore) is a numerical wave model to obtain realistic estimates of wave parameters in coastal areas, lakes and estuaries from given wind- , bottom and current conditions.

SWAN is a third-generation fully spectral model (no a priori spectral constraints).

The theoretical background, in particular the numerics, of the model is described in Holthuijsen et al. (1993) and Ris et al. (1994).

Action energy balance

SWAN is based on the notion of a spectral action balance which in the absence of a mean current reduces to an energy balance.

The action density is equal to the energy density divided by the relative frequency: $N(\sigma,\theta) = E(\sigma,\theta)/\sigma$. The rate of change of action density is described by the spectral action conservation equation (Whitham, 1974; Phillips, 1977; Mei ,1983; Hasselman et al., 1973):

$$\frac{\partial}{\partial t}N(\sigma,\theta) + \frac{\partial}{\partial x}c_x N(\sigma,\theta) + \frac{\partial}{\partial y}c_y N(\sigma,\theta) + \frac{\partial}{\partial \sigma}c_\sigma N(\sigma,\theta) + \frac{\partial}{\partial \theta}c_\theta N(\sigma,\theta) = \frac{S(\sigma,\theta)}{\sigma}$$

in which the first term in the left-hand side of the equation represents the rate of change of action in time, the second and third term represent propagation of action in geographical space (with propagation velocities c_x and c_y respectively). The fourth term represents shifting of the relative frequency due to variations in depths and currents (with propagation velocity c_σ). The fifth term represents propagation in directional space (refraction) due to depth and current induced refraction (with propagation velocity c_θ). In SWAN the situation is considered to be stationary so that the first term is removed (quasi-stationary computations can be carried out by using a sequence of SWAN computations).

The term $S(\sigma,\theta)$ at the right hand side of the balance equation is the source term in terms of energy density. This source term can be written as the sum of a number of separate source terms, each representing a different type of process:

$$S(\sigma,\theta) = S_{in}(\sigma,\theta) + S_{nl}(\sigma,\theta) + S_{ds}(\sigma,\theta),$$

where S_{in} is the growth of wave energy by wind (Snyder et al., 1981; Janssen, 1989, 1991), S_{nl} is the wave energy transfer due to nonlinear wave-wave interactions, both quadruplets (Hasselmann, 1962, 1963a, 1963b) and triads (Eldeberky and Battjes, 1995) and S_{ds} the decay of wave energy due to three different processes, i.e. bottom friction $S_{ds,b}$ (Hasselmann et al., 1973 JONSWAP); Collins, 1972; Madsen et al., 1988), whitecapping $S_{ds,w}$ (Hasselmann, 1974; Komen et al., 1984; Janssen, 1991) and depth-induced wave breaking $S_{ds,brk}$(Battjes and Janssen; 1978).

In summary SWAN can model the following effects:

- propagation in x,y direction
- generation by wind
- dissipation by whitecapping
- dissipation by depth-induced wave breaking
- dissipation by bottom friction
- redistribution of wave energy over the spectrum by non-linear wave-wave interactions (quadruplets and triads)
- refraction by bottom- and current variations
- shoaling due to bottom- and current variations
- wave-current interactions (frequency shifting, energy exchange blocking and reflections)

SWAN does not model the effects of wave diffraction, therefore results should be interpreted with caution behind coastal structures and on other locations where large gradients in the wave height occur. At a larger distance behind such locations the neglect of diffraction effects is usually less severe, because local wave growth and the effect of directional spreading become more important.

Further SWAN is in its present state stationary in the sense that the basic formulations do not include time variations and that the physical driving forces and boundary conditions are assumed to be stationary. This means that SWAN can be used only for waves with a relatively short residence time in the computational area under consideration. A quasi-stationary approach can be taken by performing stationary SWAN computations in a time-varying sequence of boundary conditions.

The depth and currents (if present) must be given to SWAN before computations are carried out. So wave set-up cannot be taken into account by SWAN in a dynamic manner (i.e. wave induced set-up or currents cannot be computed simultaneously with waves in SWAN). In principle however an (iterative) procedure can be employed in which set-up and currents are computed alternating with waves. The set-up and currents should then be computed with a 2-dimensional flow model (not in SWAN) using the radiation stresses determined with SWAN.

SWAN computes the variations of energy density by integrating the local effects of wind, whitecapping, wave-interactions, bottom and currents while propagating with these quantities at the group velocity across a regular rectangular grid in the area of interest. The physical processes mentioned above are addressed separately in the following sections below.

Kinematics

From the linear theory the propagation velocities in geographical space and spectral space (frequency and direction), can be obtained from the kinematics of a wave train (Whitham, 1974; Mei, 1983):

$$\frac{d\underline{x}}{dt} = \underline{c_g} + \underline{U} = \frac{1}{2}\left[1 + \frac{2kd}{\sinh 2kd}\right]\frac{\sigma \underline{k}}{k^2} + \underline{U}$$

$$\frac{d\sigma}{dt} = c_\sigma = \frac{\partial \sigma}{\partial d}\left[\frac{\partial d}{\partial t} + \underline{U}\cdot\nabla d\right] - c_g \underline{k}\cdot\frac{\partial \underline{U}}{\partial s}$$

$$\frac{d\theta}{dt} = c_\theta = -\frac{1}{k}\left[\frac{\partial \sigma}{\partial d}\frac{\partial d}{\partial m} + \underline{k}\cdot\frac{\partial \underline{U}}{\partial m}\right]$$

in which d is water depth, $\underline{U}$ is current velocity and $\underline{c_g}$ is the group velocity of the waves, s is the space coordinate in the propagation direction of θ and m is a coordinate perpendicular to s. The operator d./dt denotes the total derivative along a spatial path of the energy propagation, and is defined as:

$$\frac{d}{dt} = \frac{\partial}{\partial t} + (\underline{c_g} + \underline{U}) \cdot \nabla_x$$

Wind input

The growth rate of a wave component is commonly described by:

$$S_{in}(\sigma,\theta) = A + BE(\sigma,\theta)$$

in which A describes linear growth and B exponential growth. The linear growth term is small and only contributes to the initial stage of wave growth. It is used in SWAN mainly to ensure wave growth if no initial wave energy is present. If some wave energy is present the exponential growth term becomes dominant. The effect of currents on wind generation is included by using the apparent local wind speed and direction (i.e. relative to the mean current) in the formulations of the source terms.

In 1st and 2nd generation mode in SWAN the value of A is given by an expression due to Cavaleri & Malanotte-Rizzoli (1981), in 3rd generation mode a version of the expression due to Tolman is used (1992):

For the value of B in 1st and 2nd generation mode the expression of Snyder et al. (1981) is used. In the 3rd generation mode the user can choose between the expressions of Komen et al. (1984) and Janssen (1989,1991).

Bottom friction

The energy dissipation due to bottom friction in SWAN is described by three different expressions. Available in SWAN are the expressions of Hasselmann et al.(1973, JONSWAP), Collins (1972), and Madsen et al. (1988). These expressions can all be expressed as:

$$S_{ds,b}(\sigma,\theta) = -C_{bottom} \frac{\sigma^2}{g^2 \sinh^2(kd)} E(\sigma,\theta)$$

The bottom friction coefficient C_{bottom} generally depends on the bottom orbital motion represented by $\hat{U}_{rms}$:

$$\hat{U}_{rms}^2 = \iint \frac{\sigma^2}{\sinh^2(kd)} E(\sigma,\theta) d\sigma d\theta$$

The effect of a mean current on bottom friction is not taken into account in SWAN. The reasons for this are given in Tolman (1992b) who argues that the state-of-the-art expressions for this vary too widely in their effects to be acceptable.

Whitecapping

The whitecapping dissipation source term represents the process by which energy is lost through deep water breaking. The whitecapping dissipation is controlled primarily by the limiting steepness of the waves. In 1st and 2nd generation mode there is no explicit formulation for whitecapping (it is implicitly included in the wind input formulation). In 3rd generation the user can choose between Komen et al. (1984) and Janssen (1991).

Depth-induced breaking

In SWAN a spectral version of the depth-limited part of the Battjes-Janssen wave breaking model is used. It does not affect the shape of the spectrum itself (Beji and Battjes, 1993; Battjes et al., 1993). The expression is:

$$S_{ds,br}(\sigma,\theta) = -\frac{\alpha_{BJ} Q_b \bar{\sigma} H_m^2}{8\pi} \frac{E(\sigma,\theta)}{E_{tot}}$$

in which α_{BJ} is a numerical constant of the order one.

Nonlinear wave-wave interactions

- Quadruplets interactions:

The quadruplet wave-wave interactions are computed with the Discrete Interaction Approximation (DIA, of Hasselmann and Hasselmann, 1985).

If a set of four waves fulfills a given resonance condition then they exchange energy and energy is redistributed in the energy density spectrum. The quadruplets occur in deep and intermediate water depths.

- Triad interactions:

In very shallow water the triad interactions become dominant. These interactions are of significant importance in shallow water where energy is transferred to higher frequencies, resulting in higher harmonics (Beji and Battjes, 1993). The expression in SWAN is based on the expression of Eldeberky and Battjes (1995).

Propagation in x,y direction

In SWAN wave propagation is computed for each of the wave components. This propagation is a rectilinear propagation as well as refraction and nonlinear propagation along the frequency axis.

In table 2-1 the standard settings for the 2nd and 3rd generation mode in SWAN Cycle 1 are given.

		2nd	3rd
Linear wind growth:	Cavaleri & Malanotte-Rizzoli (1981) [modified]	x	
	Cavaleri & Malanotte-Rizzoli (1981)		x
Exponential wind growth	Snyder et al. (1981) [modified]	x	
	Snyder et al. (1981)		x
Whitecapping	Holthuijsen and de Boer (1988)	x	
	Komen et al. (1984)		x
Quadruplet interaction	Hasselmann et al. (1985)		x
Triad interaction	Elderberky & Battjes (1995)	x	x
Depth-induced breaking:	Battjes & Janssen (1978)	x	x
Bottom Friction	Hasselmann et al. JONSWAP (1973)	x	x

table 2-1 Standard settings SWAN Cycle 1 (20.87) for 2nd and 3rd generation mode

2.2.3 HISWA

The model HISWA (which is an acronym for HIndcast Shallow Water WAves) is, like SWAN, a numerical model to obtain realistic estimates of wave parameters in coastal areas, lakes and estuaries from given stationary wind-, bottom-, and current conditions. The model is also based on a parametrized version of the action balance of waves.

Unlike SWAN, HISWA is not a fully spectral model. In HISWA the spectrum is discrete spectral only in the directions. In the frequencies HISWA is parametric, in each spectral direction two quantities are propagated: a frequency integrated energy density and a mean frequency. HISWA computes this propagation by integrating the local effects of wind, bottom and currents while propagating with these quantities at the group velocity of the mean frequency across a grid in the area of interest. The computations are carried out for each wave component separately on the basis of two evolution equations.

- an evolution equation for the zeroth order moment of the action density spectrum for each spectral direction.

$$\frac{\partial}{\partial x}\left(c_x^{*}A_0\right)+\frac{\partial}{\partial y}\left(c_y^{*}A_0\right)+\frac{\partial}{\partial \theta}\left(c_\theta^{*}A_0\right)=T_0$$

- an evolution equation for the first order moment of the action density spectrum for each spectral direction

$$\frac{\partial}{\partial x}\left(c_x^{**}A_1\right)+\frac{\partial}{\partial y}\left(c_y^{**}A_1\right)+\frac{\partial}{\partial \theta}\left(c_\theta^{**}A_1\right)=T_1$$

A_0 and A_1 are the zeroth and first order moments of the action density spectrum in each spectral direction. The left hand side of these equations represents propagation of the waves where c_x^{*}, c_y^{*}, c_θ^{*} are the propagation speeds of action in x- y- and θ- space respectively. Similarly c_x^{**}, c_y^{**}, c_θ^{**} are the propagation speeds of the mean frequency in x- y- and θ- space respectively. The propagation speeds c_x, c_y represent rectilinear propagation whereas c_θ represents refraction. Generation and dissipation of A_0 and A_1 are represented by the source terms T_0 and T_1 respectively.

In summary HISWA can model the following effects:

- propagation in x,y direction
- generation by wind
- dissipation by bottom friction
- dissipation by depth-induced wave breaking and added whitecapping
- dissipation by currents

HISWA does not model the effects of wave diffraction. Results should be interpreted with caution behind coastal structures. At a larger distance behind such locations the neglect of diffraction effects is usually less severe.

Propagation in x,y direction

In HISWA wave propagation is computed for each of the wave components described above. In the basic evolution equations of HISWA (see above), this propagation is separated in rectilinear propagation and refraction.

Rectilinear propagation:

Represented by c_x and c_y gives propagation in x,y space based on linear wave theory, including bottom and current induced shoaling. These propagation speeds are determined with the mean frequency (different for each spectral direction).

Refraction:

HISWA computations are based on a grid rather than the conventional wave-ray approach. So refraction is accounted for by shifting energy from one direction to another during propagation. This is expressed in the basic evolution equation of HISWA with the speed c_θ.

Wind growth

The wind induced development of the wave energy and the mean frequency are considered for each spectral wave direction separately and independent from other spectral directions. The formulations are taken from empirical information in an idealized situation (unlimited ocean with homogeneous and stationary wind), under the assumption that in that situation the directional energy distribution has a universal shape.

$E^{\cdot}_{tot} = A * (t^{\cdot})^B \qquad t^{\cdot} < t^{\cdot}_{max}$

$E^{\cdot}_{tot} = A * (t^{\cdot}_{max})^B \qquad t^{\cdot} >= t^{\cdot}_{max}$

and

$f^{\cdot}_{av} = P * (t^{\cdot})^Q \qquad t^{\cdot} < t^{\cdot}_{max}$

$f^{\cdot}_{av} = P * (t^{\cdot}_{max})^Q \qquad t^{\cdot} >= t^{\cdot}_{max}$

where $E^{\cdot}_{tot}$ is the dimensionless total energy, $f^{\cdot}_{av}$ the dimensionless average frequency, $t^{\cdot}$ the dimensionless time and $t^{\cdot}_{max}$ the dimensionless time at which the maximum energy is reached. All these variables are made dimensionless with the mean wind velocity at 10 m elevation (U_{10}) and the gravitational acceleration g. These formulations are transformed in HISWA to formulations in space with the default values of coefficients A, B, P, Q and $t^{\cdot}_{max}$ in HISWA chosen such that the HISWA results for fetch limited growth (significant wave height and significant period) are reasonable approximations of standard growth curves.

The evolution of the mean period per spectral wave direction is based in HISWA on an assumed universal relationship between the total wave energy and the overall mean frequency (in dimensionless form).

Bottom dissipation

In shallow water some wave energy is dissipated in HISWA by bottom friction. This dissipation is determined with a fairly conventional non-linear bottom friction formulation including the effect of a mean current. It is based on a conventional formulation for periodic waves adapted to suit a random wave field in an ambient current field.

$S(\theta) = - U^2_{bot1} * [c_{fw} * U_{bot2} + c_{fc} * U_{cur}]/g$

Where c_{fw} and c_{fc} are the friction coefficients for the waves and currents respectively, U_{bot1} and U_{bot2} are measures for the orbital movement at the bottom, U_{cur} is the current velocity in the direction of θ and g is the gravitational acceleration.

The mean frequency per spectral wave direction is affected by bottom friction in HISWA assuming that the wave dissipation due to bottom friction affects only energy at low frequencies.

Surf dissipation and added whitecapping

In extremely shallow water or if a certain wave steepness is exceeded (in deep or shallow water), the waves will break. The corresponding energy dissipation is determined in HISWA with a bore-model (Battjes Janssen 1979) for those waves which are higher than a threshold value. Only the total rate of energy dissipation is thus determined. The total energy obtained is distributed over the wave directions proportional to the existing directional energy distribution. The directional characteristics of the waves in HISWA are therefore not affected by breaking.

The mean frequency is not affected in HISWA in the case of steepness induced breaking. In the case of bottom induced breaking, the mean frequency is affected in the same way as by bottom friction.

The effect of a mean current on surf breaking is not taken into account. Whitecapping is affected by a mean current in HISWA through the influence on the wave number k.

Blocking

In a strong adverse current some wave energy is carried away by the current. This is energy which in a fully spectral model (like SWAN) is carried by wave components which cannot travel against the current (propagation speed less than current speed). This energy is removed from the wave field in the HISWA model through high frequency dissipation.

For the computation of the current dissipation for a directional component, a critical frequency f_c is determined. This is the lowest frequency that cannot travel against the current. In HISWA the energy carried by the frequencies higher than the critical frequency is assumed to be dissipated. If the waves propagate against an increasing opposing current, the critical frequency f_c decreases and the high-frequency energy decreases accordingly. This dissipation is equal to the decrease of total energy of the following spectrum as the critical frequency decreases:

$E(f, \theta) = C(\theta) * f^{-n}$ for $f > f_{peak}$

$E(f, \theta) = 0$ for $f < f_{peak}$ and $f > f_c$

with a constant $C(\theta)$

3 Data-set

3.1 Origin of data

Within the scope of the HYDRA project two case studies are set up. One is conducted in the Dutch coastal town Petten which will be exemplary for the closed coastline of the Netherlands.

Petten is situated in the province Noord Holland. The coast is characterized by nearly straight depth contours with a bar and a trough. Further offshore (3 km) an offshore bank called the 'Pettemer Polder' is situated. Wave measurements were already taken here in the past. So, part of the infrastructure needed for the new measurements was already present at the Petten location. Another reason to choose this location is the absence of heavy shipping traffic because of the 'Pettemer polder'. The measuring buoys have little chance being destroyed by ships.

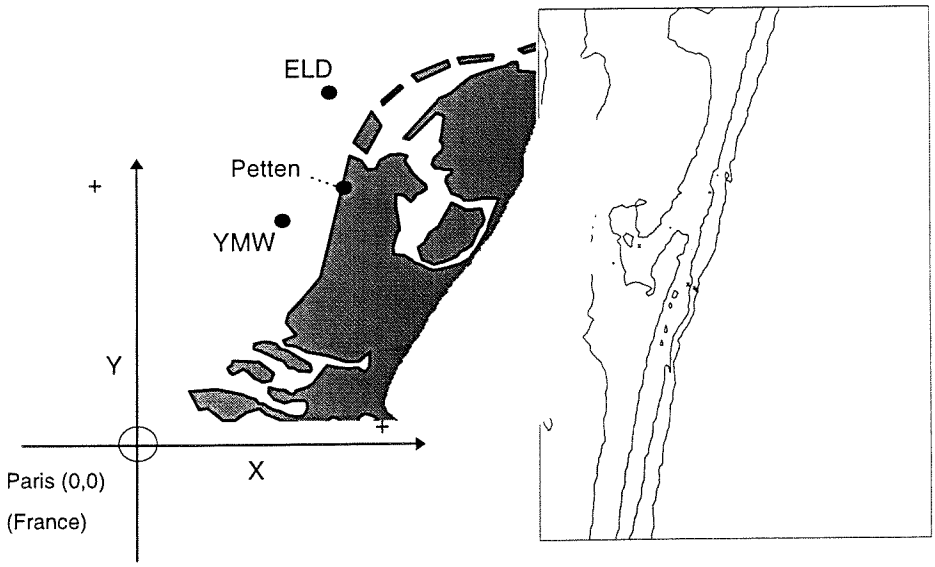

figure 3-1 **Location Petten coastal area with measuring stations 'Eierlandse Gat' (ELD) and 'IJmuiden' (YMW)**

In the 'Petten' measuring campaign seven measuring points (besides permanent stations ELD and YMW) positioned in one a straight line perpendicular to the coast were used (figure 3-1, figure 3-2). The first at deep water is a WAVEC directional waverider placed 8.3 km offshore to measure the incoming waves and their directions (Mp1). Closer to the coast at about 3500 m offshore a waverider is placed to measure the waves at the deep water side of the 'Pettemer Polder' (Mp2). Next is a measuring pole situated 635 m offshore. On this measuring pole there is a wave staff and water level meter (Mp3). Next to this measuring pole

there is a waverider (Mp4) to compare the results from the wave staff with the results of this waverider. Nearshore the bank another directional waverider is placed (Mp5) at 300 m offshore . In the very shallow part in front of the sea dike (130 m) a measuring pole (Mp6) is situated with which the surface elevation and windspeed and directions are recorded. Next to this pole a pressure transducer is placed to have a double check. The last measuring point is placed on the dike slope to measure the wave run-up (Mp7).

The location of the measuring devices and their names are given in table 3-1. The abbreviation NAP means Normaal Amsterdams Peil (mean sea level).

Wave sensor	Code	Bottom elevation NAP (m)	Distance to dike top (m)	Paris Coordinate X (km)	Paris Coordinate Y (km)
Wavec Buoy	ELD	26.0	48000	101.528	579.567
Wavec Buoy	YMW	21.0	47000	065.344	507.662
Dir. Waverider	Mp1	20.0	8300	098.981	536.444
Waverider	Mp2	10.0	3500	103.000	533.800
Wave staff Water level meter	Mp3	8.0	635	105.230	531.990
Waverider	Mp4	8.0	625	105.250	532.000
Dir. Waverider	Mp5	8.5	300	105.520	531.830
Wave staff	Mp6	2.2	150	105.650	531.746
Pressure transducer	Mb6	2.2	150	105.650	531.746
Wind meter	Mw6	2.2	150	105.650	531.746
Wave run-up gauge	Mp7	-5.8 : -9.0	20	105.744	531.686

table 3-1 Location of wave sensors

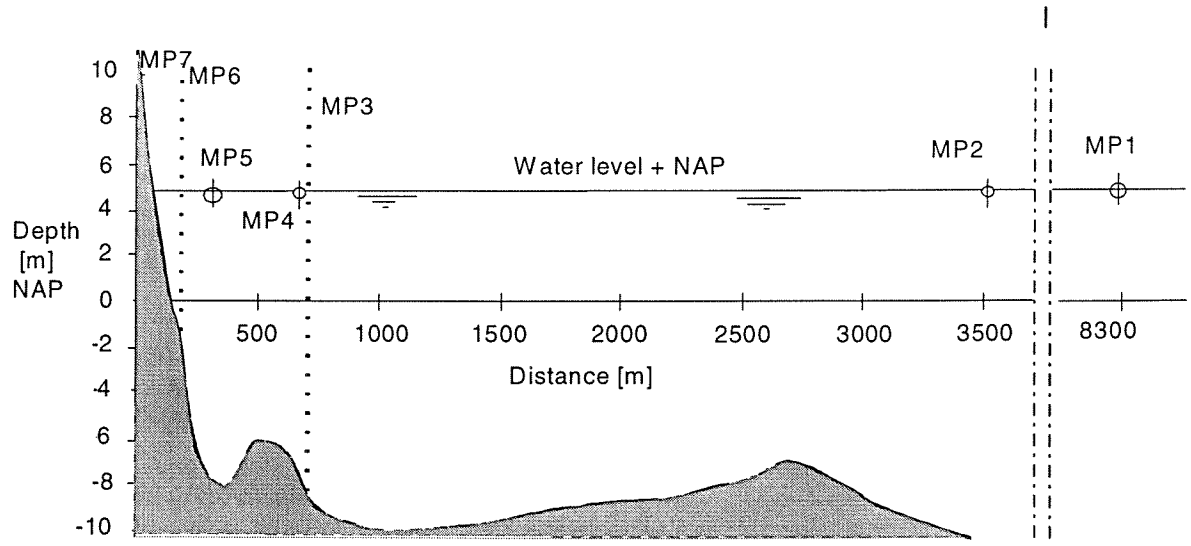

figure 3-2 Depth profile with location of wave sensors

The data acquired at these locations was stored in data files and sent to RIKZ for the calculation of relevant parameters from these data. Which parameters are relevant is decided upon in the contents of the HYDRA-project.

3.2 Quality of data

The processing of the data files was done by J.H. Andorka Gal of the RIKZ. The results are described in Verification set Petten [Andorka 1996]. This document presents histories of wave parameters and energy density spectra. Some remarks have to be made concerning the data set from January 1995.

- During the measurement campaign in January of 1995 the Waverider at Mp4 (see table 3-1) was damaged and did not send any data.
- The wavestaff located at measuring pole Mp6 was placed too high above mean sea level so for low waterlevels there is no registration of the smaller waves.
- The pressure transducer Mb6 is not able to register the surface elevation directly. So the energy density spectrum has to be calculated from the pressure time series. The pressure consists of a hydrostatic and a dynamic part. The hydrostatic part is related to the mean water level above the sensor. The dynamic part is caused by the motion of waves. The dynamic part of each wave component decreases with depth according to:

$$p_{dyn} = \frac{\rho g H}{2} \frac{\cosh(k(z+h))}{\cosh(kh)} \cos(kx - \omega t)$$

with

p_{dyn}	= subsurface pressure z [m] above bottom (dynamic part)	[Pa]
ρ	= density	[kg/m^3]
H	= wave height	[m]
h	= total water depth	[m]
z	= height above still water level	[m]
k	= wave number = $2\pi/L$	[m^{-1}]
L	= wave length	[m]
ω	= angular frequency	[rad/s]

in which wave lengths L are related to periods (thus frequencies) according the dispersion relation:

$$\left(\frac{L}{T}\right)^2 = \frac{gL}{2\pi} \tanh\left(\frac{2\pi h}{L}\right)$$

The spectrum determined from the pressure transducer time series is related to a free surface elevation spectrum by correcting the energy density for each frequency.

$$E_{hh}(f) = (\rho g)^{-2} \left[\frac{\cosh(kh)}{\cosh(k(h+z))}\right]^2 E_{pp}(f)$$

with

$E_{\eta\eta}(f)$	= spectral density of free surface elevation at frequency f	[m^2/Hz]
$E_{pp}(f)$	= spectral density of pressure at frequency f	[Pa^2/Hz]

Because of this adaptation the error in the energy density for high frequencies will be extremely overestimated. The maximal frequency for which this adaptation is thought to be still valid in shallow water conditions is 0.30 Hz [Ruessink (1995)].

As in any other measurement errors are made. The error made in the spectral density for the frequencies just below 0.30 Hz is amplified most, so special caution has to be taken into account when using parameters from Mb6.

3.3 Selection of data

To select data from the measurements of two independent storms of January 1995 the following selection criteria were used.

- high wave run-up
- different spectral shapes
- data from both storms
- availability of data for as many measuring positions as possible.

Three situations to be modeled are selected from the wave records of the 1st,2nd and 10th of January 1995, because the first storm can be divided into two (related) storms (figure 3-4). By selection three situations all three storm data are covered. For station Mp1 the main parameters for these times are presented in table 3-2.

Date		Jan 1st 1995	Jan 2nd 1995	Jan 10th 1995
Time	[h.] (U.T.C.)	16:00	04:00	11:00
Waterlevel	[m] (+NAP)	2.10	2.30	2.03
Hs	[m]	4.61	5.05	4.57
Mean wave direction	[degree] (α)	219	325	321
Tp	[s]	10.00	11.1	14.29
Tm_{01}	[s]	8.37	8.96	8.63
Wind speed	[m/s]	16.1	17.1	13.7
Wind direction	[degree] (α)	292	323.5	274

table 3-2 Selected data for computations (data for station Mp1)

(α) means according nautical convention

In the three figures below the wind speed record is presented. The records have a length of 2:20 hours, lasting from 2 hours before, until 20 minutes after the selected times.

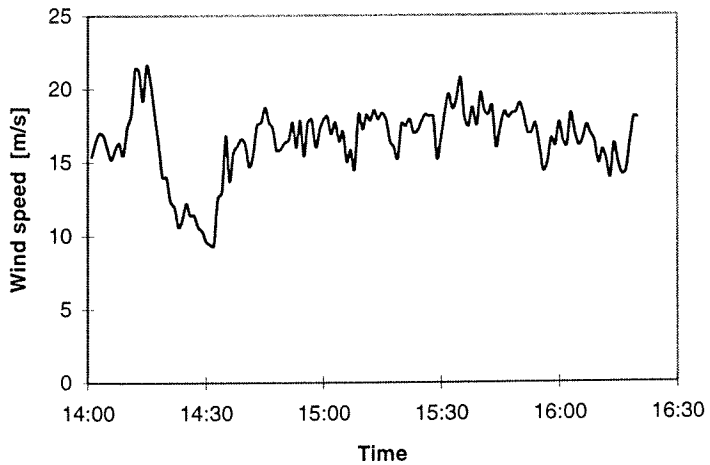

figure 3-3 **Wind speed record at 1-1-1995 from 14:00 to 16:20 (U.T.C.)**

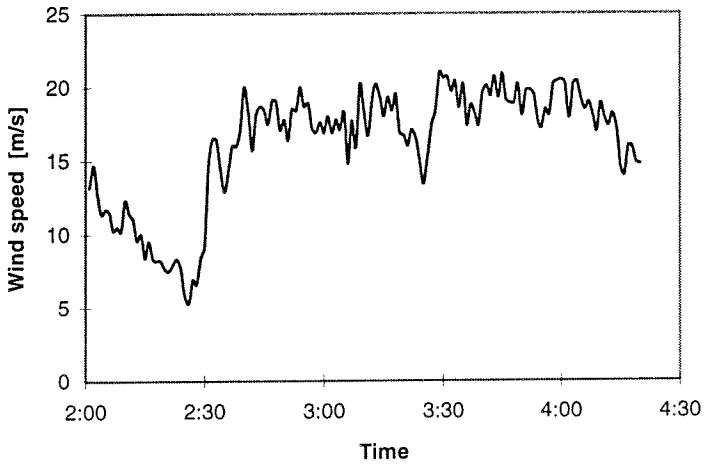

figure 3-4 **Wind speed record at 2-1-1995 from 02:00 to 04:20 (U.T.C.)**

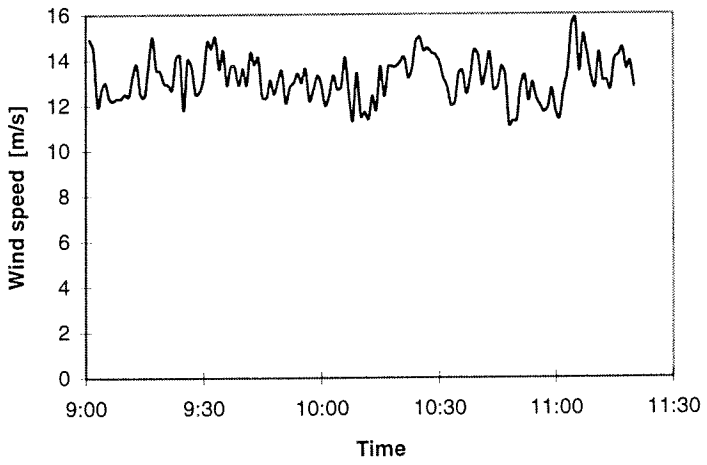

figure 3-5 **Wind speed record at 10-1-1995 from 09:00 to 11:20 (U.T.C.)**

The wind speed records for case 1 and 2 show a decrease followed by an increase in wind speed 1:30 hours before the selected times. The wind speed record for case 3 shows a fairly constant wind speed.

3.4 Bathymetry

An important part in the numerical wave modeling is an appropriate bottom schematization. The bathymetry used in this study is composed from several different sources, interpolated with the tool Digipol. Digipol is a computer program which interpolates x,y,z data files to a spatial matrix. Digipol is able to recognize trenches and troughs in digitized sounding data. It will produce a bottom depth matrix which is oriented East-West (x-axis) North-South (y-axis) with an equidistant grid.

The following digitized sounding data are used to compose the appropriate bottom schematizations:

- H1883_bottom_h2 A matrix with depth values used by Delft Hydraulics in 'Extreme wave conditions along the coast of the Netherlands'. These data are obtained from echo sounding of the Dutch Navy and irregularly spaced data of the 'Kuststrook model' [Dekker,Hartsuiker (1995)]
- lod21119.asc - Sounding data measured in September/October 1994 of the sea area around the Pettemer polder. This sounding is done in rays perpendicular to the coastline. The area covered is situated between km 18.000 and km 24.000 till about 10 km offshore.
- detl2109.asc - Detailed sounding data of the Pettemer sea defense measured on the 21st of September 1994 between km 20.000 and km 22.000.
- dijk.xyz - Profile of the Pettemer sea dike which is shifted along the dike-top.

The bottom schematizations used differ in size and resolution. Three schematizations with increasing resolution for more detailed information nearshore are made:

- Petten12.asc A coarse grid composed from H1883_bottom_h2 and lod21119.asc (figure 3-6). Resolution 500 m x 500 m.
- Petten234.asc A fine grid composed from H1883_bottom_h2, lod21119.asc and detl2109.asc (figure 3-7). Resolution 50 m 50 m.
- Petten34.asc A super fine grid composed from lod21119.asc and detl2109.asc (figure 3-8). Resolution 5 m x 5 m.

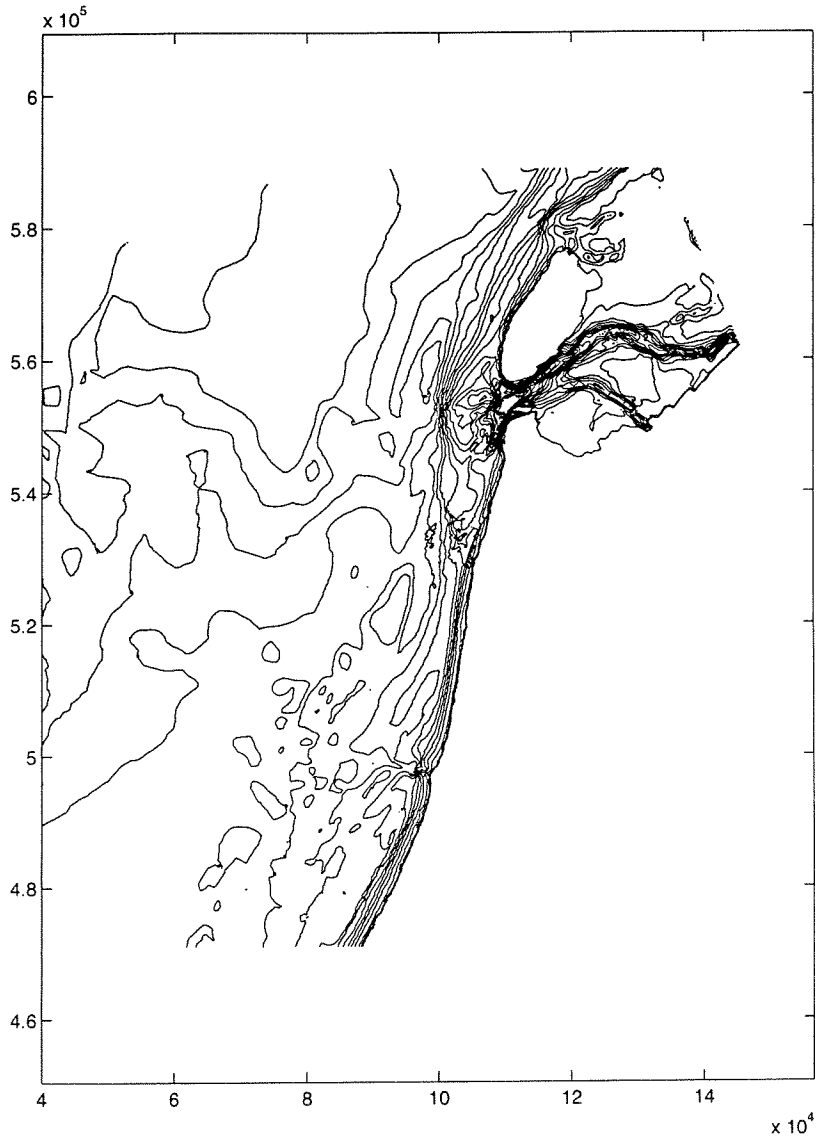

figure 3-6 Coarse (500 x 500 m) grid Petten12.asc

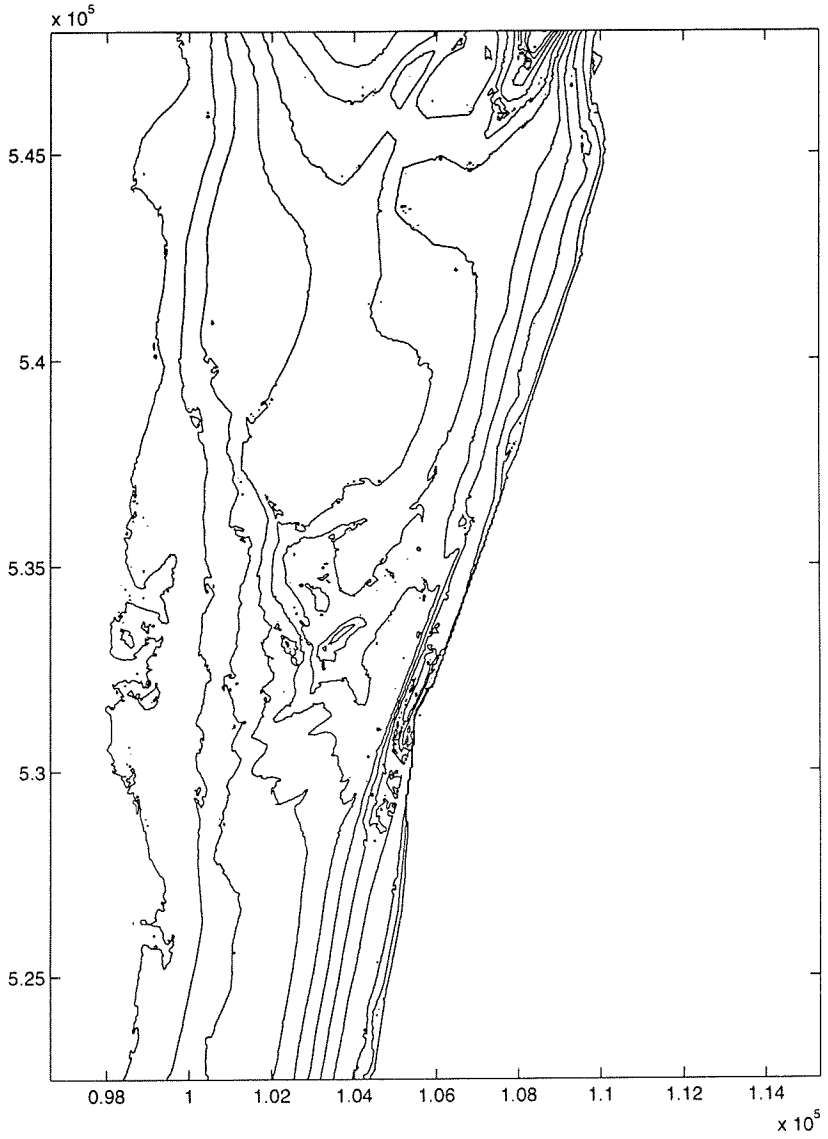

figure 3-7 Fine (50x 50 m) grid Petten234.asc

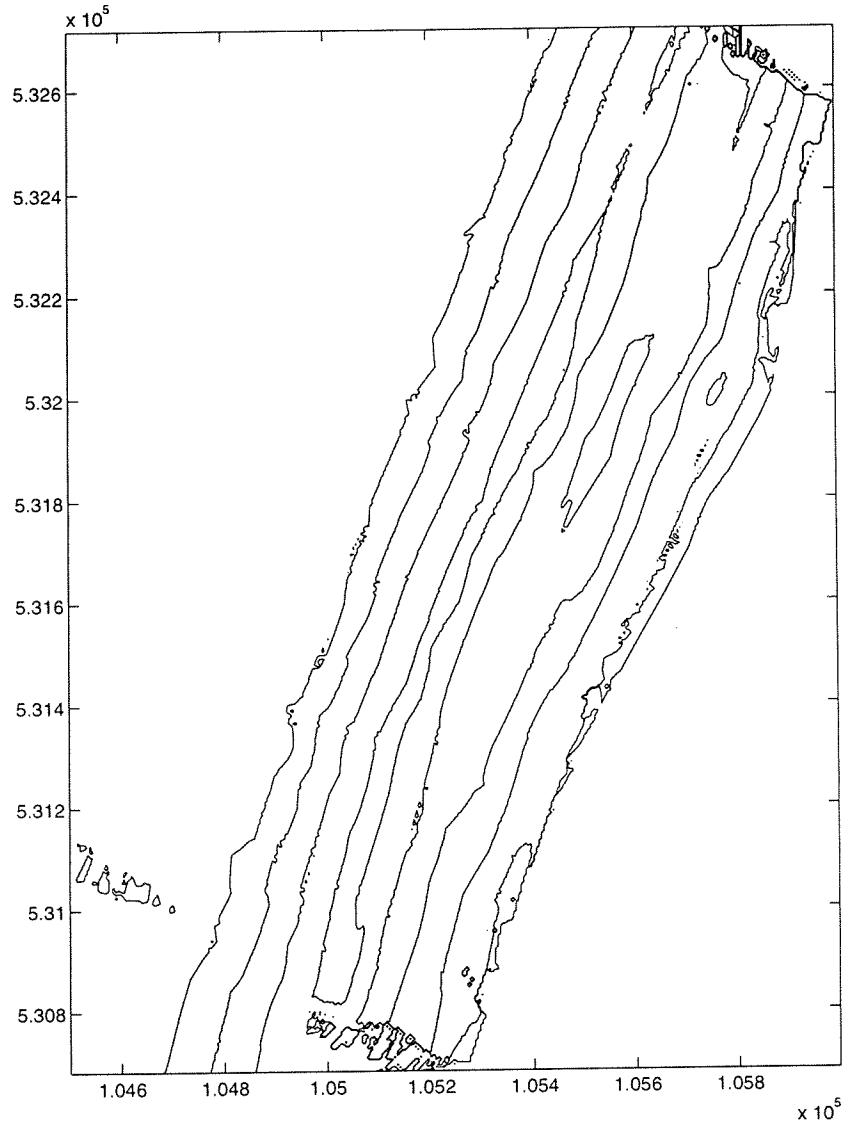

figure 3-8 **Super fine (10x 10 m)** **Petten34.asc**

4 SWAN applied to the Petten area

4.1 Base cases

The size and orientation of the grids needed for a SWAN computation can be decided upon in several ways. One of which is the approach of the RIKZ who want to give a predictions of nearshore wave conditions from permanent offshore measurement stations where they have wave data and statistics (approach 1). So the wave model can be used in a operational system to predict wave conditions nearshore from one of the permanent offshore stations.

Another approach is that of the researcher who wants to verify the numerical wave model, so the offshore boundary conditions have to be as accurate as possible (approach 2). The stations in the measuring campaign of 1995 are placed so that they are perpendicular the coastline. The wave conditions measured are from one stationary situation.

Both these approaches will be compared in the next sections.

The coordinate system used throughout this report is the geodetic system of the Netherlands (Paris coordinates). In this system spherical earth coordinates are transferred to a flat plane. The flat plane is situated over the Netherlands with its origin in Amersfoort. To the coordinates of this plane the coordinates from Amersfoort to Paris are added. The Y-axis is pointing to the North and the positive X-axis is in easterly direction. The rotation angle (α) is positive clockwise measured from the positive Y-axis.

4.1.1 Approach 1

This first approach is the approach used by the RIKZ.

Orientation and size of grids

Two permanent offshore measuring stations provide for the offshore wave boundary conditions for an outer model. The grid of this outer model has its offshore boundary near two offshore stations ELD and YMW. The grid measures 35 km by 80 km. Its origin is at the location of offshore measuring station YMW and rotated 26.71° clockwise measured from the positive Y-axis. This model supplies boundary conditions for a smaller model. The grid of this model measures 12.5 km by 20 km. Its offshore boundary is near the 20 meters depth contour. The rotation is 5° clockwise measured from the positive Y-axis. This fine model in its turn supplies the wave boundary conditions for the super fine model near the Petten sea dike. The grid of this model measures 1 km by 2 km and has a very high resolution, because of the variation in bottom topography. The rotation of this super fine grid is 15° clockwise measured from the positive Y-axis (figure 4-1 , table 4-1).

Boundary conditions

The offshore boundary wave conditions are supplied by the measuring stations ELD and YMW. A spectrum is estimated from the data of these two stations that is representative for the wave conditions between the two stations. This estimation is done by averaging the energy densities, the directions and the directional spreading from the spectra of the two offshore stations (ELD and YMW) and using this averaged spectrum as the offshore boundary wave condition for the outer model.

This outer model creates the boundary conditions for the fine model which in its turn provides for the boundary conditions for the super fine model (nesting). This nesting is done because the variation in bottom topography is more important near shore.

The wind conditions are recorded at station Mp6 (table 3-1) and taken to be uniform over the entire modeled area. The water level is taken from measurements at station Mp3 and taken to be uniform over the entire modeled area (i.e. no wave set-up).

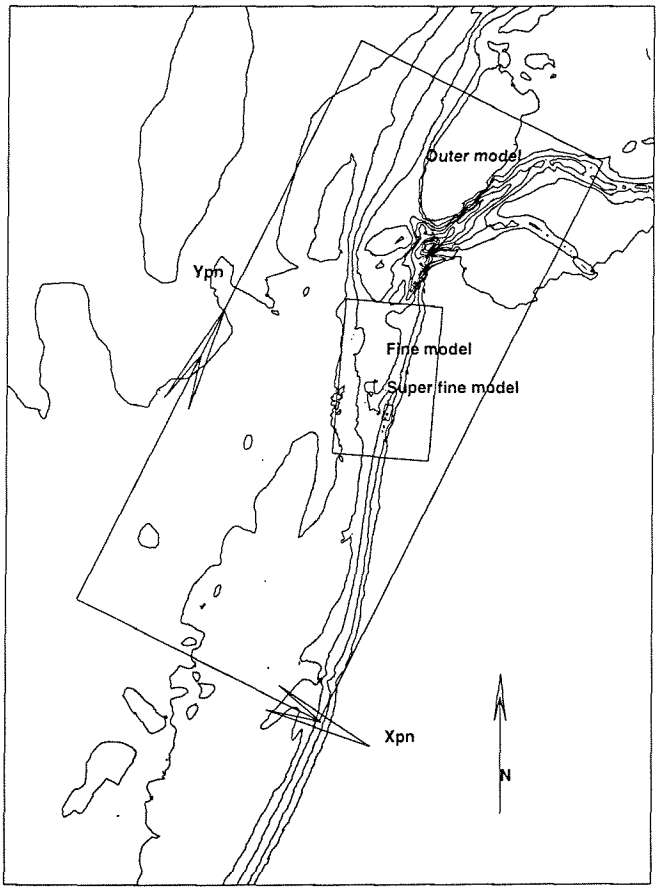

figure 4-1 Orientation and size of grids of approach 1

Approach 1 name:	Outer model	Fine model	Super fine model
Area name:	Area 1	Area 2	Area 3
Origin: (Paris Coor.) [m]	65344, 507662	98105, 526480	104500, 530900
Size : [m]	35000 X 80800	12500 X 20000	1000 X 2000
Rotation : [°] clockwise	26.71	5.00	15.00
Resolution: [Δx x Δy] [m]	200 x 200	62.5 x 100	10 x 20
Resolution: [meshes]	175 X 202	200 X 200	100 X 100

table 4-1 Orientation and size of grids of approach 1

4.1.2 Approach 2

This second approach is more specific to verify the numerical wave model.

Orientation and size of grids

In this approach (approach 2) the grids are identical (location as well as grid size and orientation) to the two inner grids (fine and super fine) of approach 1. (figure 4-2, table 4-2).

Boundary conditions

The offshore boundary wave conditions are provided by measuring station Mp1 uniformly distributed over the offshore boundary. To limit the error area caused by wave propagation at the North side boundary of the model (lateral boundary) the HISWA wave model is used to estimate the wave condition variation over this boundary. These calculated wave conditions are used as a lateral boundary in the SWAN computations. This is done to limit the erroneous zone. The effect of this on the results of the Petten transect are very small (smaller than 1%). Near the dike there is no difference.

The wind conditions are recorded at station Mp6 (table 3-1) and taken to be uniform over the entire modeled area. The waterlevel is taken from measurements at station Mp3 and taken to be uniform over the entire modeled area (i.e. no wave set-up).

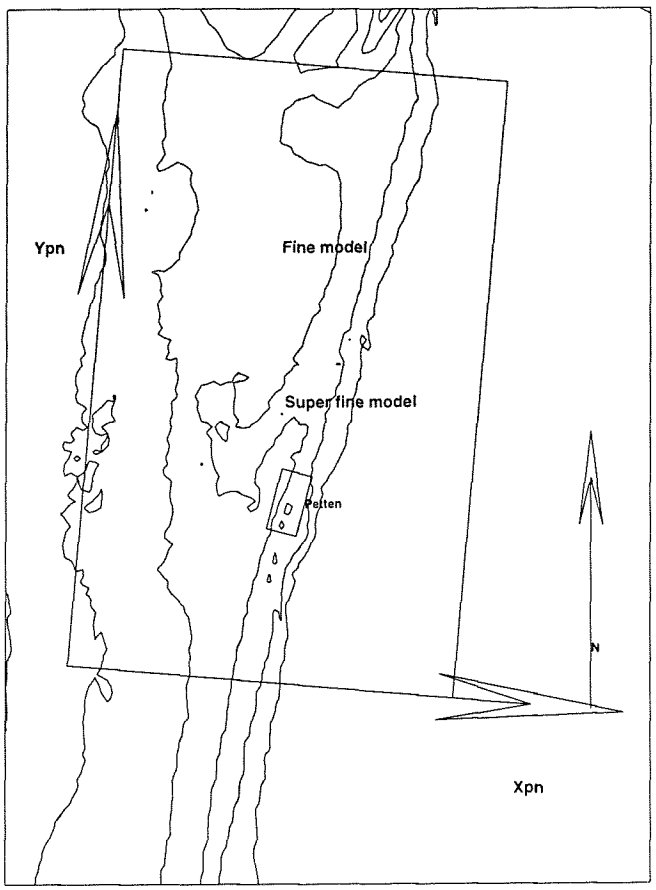

figure 4-2 Orientation and size of grids approach 2

Approach 2 name:	Fine model	Super fine model
Area name :	Area 2	Area 3
Origin: (Paris Coor.) [m]	98105, 526480	104500, 530900
Size : [m]	12500 X 20000	1000 X 2000
Rotation : [°] Clockwise	5.00	15.00
Resolution: [Δx x Δy] [m]	62.5 x 100	10 x 20
Resolution: [meshes]	200 X 200	100 X 100

table 4-2 Orientation and size of grids approach 2

4.1.3 Model settings

The computations made in this section are done with the standard settings in SWAN (table 4-3). The resolution in frequency space is taken such that the calculated spectrum resembles the input as much as possible. A small difference will always be present because the distribution of energy over the frequencies in the measurements is equidistant while SWAN uses a logarithmic distribution. The resolution in wave propagation direction space is taken 9°. The frequency boundaries are taken equal as the ones from the measuring instruments.

Linear wind growth:	Cavaleri & Malanotte-Rizzoli (1981)	
Exponential wind growth	Snyder et al. (1981)	
Whitecapping	Komen et al. (1984)	activated
Quadruplet interaction	Hasselmann et al. (1985)	activated
Triad interaction	Elderberky & Battjes (1995)	activated
Depth-induced breaking:	Battjes & Janssen (1978)	$\gamma = 0.73$, $\alpha = 1.0$
Bottom friction	Hasselmann et al. JONSWAP (1973)	$C_{f,Jonswap}=0.067$ [m^2s^{-3}]

table 4-3 Standard settings SWAN Cycle 1 (20.87)

4.2 Results of base cases

To compare the results of a SWAN computation with measurements ,it is necessary to use the same frequency range for the calculation of spectral parameters from measurements and computation. Especially wave periods are very sensitive for frequency range variations. In SWAN a diagnostic tail is added to the energy density spectrum. The values for the mean periods are slightly smaller with this tail than calculated without this tail. A tail of the same $E(f)^{-5}$ shape for frequencies above 0.5 Hz is added to the density spectrum from the measurements to eliminate this difference.

4.2.1 Comparison approach 1 and approach 2 with measurements

In approach 2 the measured spectrum at station Mp1 is used as the input spectrum for the offshore boundary of the fine model of approach 2 (figure 4-2). The input spectrum and the spectrum calculated by SWAN at this station are not exactly the same because of two reasons:

- The wave components with directions out of the computational area in SWAN need not be the same as the observed wave components.
- The measured wave spectra have a linear frequency distribution while the spectra calculated in SWAN have a logarithmic frequency distribution.

The results are presented in the figures further in this report where the right side of the figure is the offshore side and the left is the coast. The results of the fine computations are replaced by the results of the superfine model where this

superfine model exists and presented in one figure for each computation. The results for stations Mp3, Mp4, Mp5 and Mp6 are taken from the superfine models.

Case 1: January 1st 16:00 h (U.T.C.) 1995

Results from computations and the measurements of the 1st of January 1995 16:00 hours are presented in table 4-4, figure 4-4, figure 4-5 and figure 4-6.

	Measurement			Comp. approach 1			Comp. approach 2 (starting at Mp1)		
Station:	Hm_0 [m]	Tm_{01} [s]	Tm_{02} [s]	Hm_0 [m]	Tm_{01} [s]	Tm_{02} [s]	Hm_0 [m]	Tm_{01} [s]	Tm_{02} [s]
Mp1	4,61	8.22	7.30	4.44	7.65	6.75	4.55	8.17	7.23
Mp2	4.06	8.37	7.48	4.01	7.51	6.65	4.13	7.81	7.00
Mp3	3.88	6.95	6.01	3.74	7.16	6.25	3.77	7.32	6.39
Mp4				3.72	7.16	6.26	3.74	7.32	6.40
Mp5	2.67	6.86	5.91	2.89	6.85	5.95	2.88	7.00	6.09
Mp6	2.95	7.05	6.37	2.56	7.35	6.49	2.55	7.49	6.60

table 4-4 Comparison approach 1 and 2 with measurements

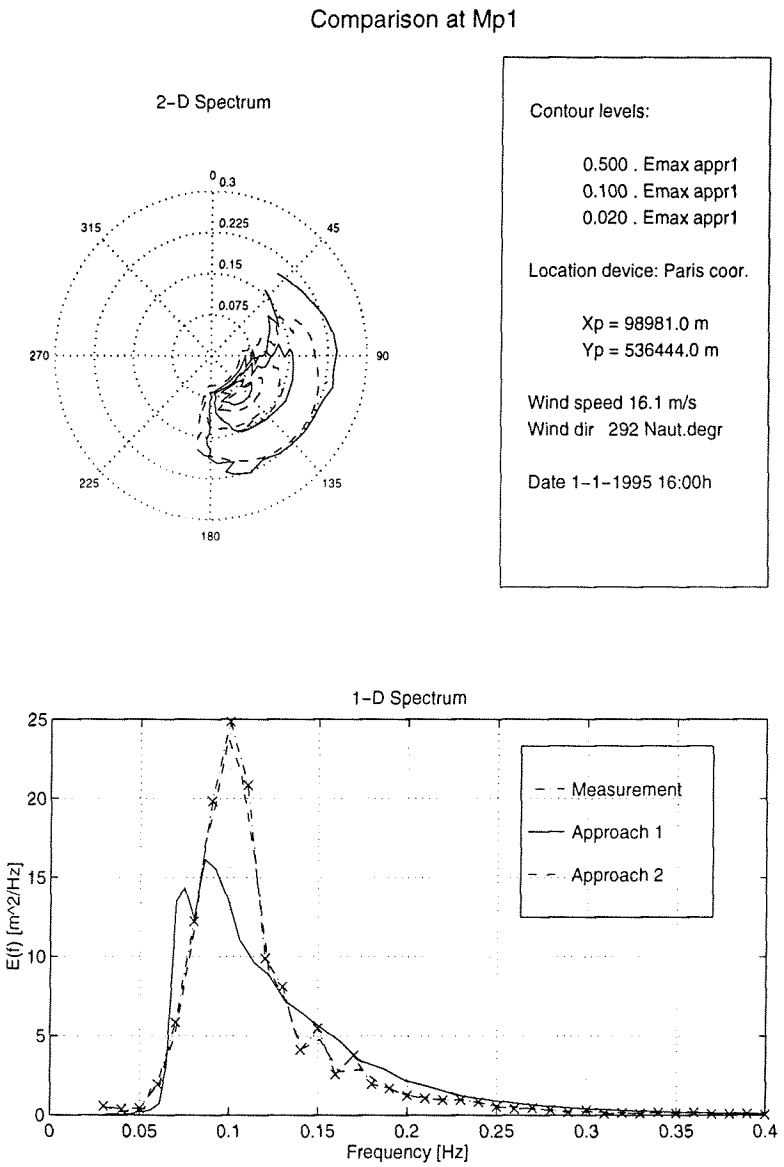

figure 4-3 **Comparison energy density spectra approach 1 and approach 2 with measurement at station Mp1 at 1-1-1995 16:00 h. (U.T.C.)**

The wave conditions for station Mp1 in approach 1 are calculated from the outer model with input conditions from station ELD only , because station YMW did not send any reliable data at this part of the day.

The differences in station Mp1 between the two approaches are not large for the wave parameters Hm_0 (2.5 % of the value of approach 2) and Tm_{02} (6.6% of the value of approach 2) (table 4-4).

The difference in Hm_0 at Mp6 (station nearest to the shore) between both approaches is 0.5 % and for the period Tm_{02} 1.7% of the value of approach 2 (figure 4-4).

The significant wave height slowly decreases from station Mp1 to about 3000 m offshore where there is a bank. Here the significant wave height decreases rapidly to about 3.5 m. From 3000 m to 1000 m offshore the depth increases from 4 m to 10 m (-NAP). Here the significant wave height increases again with some

0.20 m. At about 700 m offshore there are large gradients in the bottom profile from 10 m to 5 m (-NAP) and the significant wave height decreases rapidly over the bar and decreases further until the waves reach shore.

The mean period Tm_{02} at 8300 m offshore differs 6.5% of the value of approach 2 between the two approaches (figure 4-4). This is also seen in the energy density spectrum at the offshore boundary (figure 4-3). where both approaches have a different energy distribution, hence a different mean period. The differences are getting smaller shoreward. At Mp6 the difference in Tm_{02} is 1.5% of the values of approach 2.

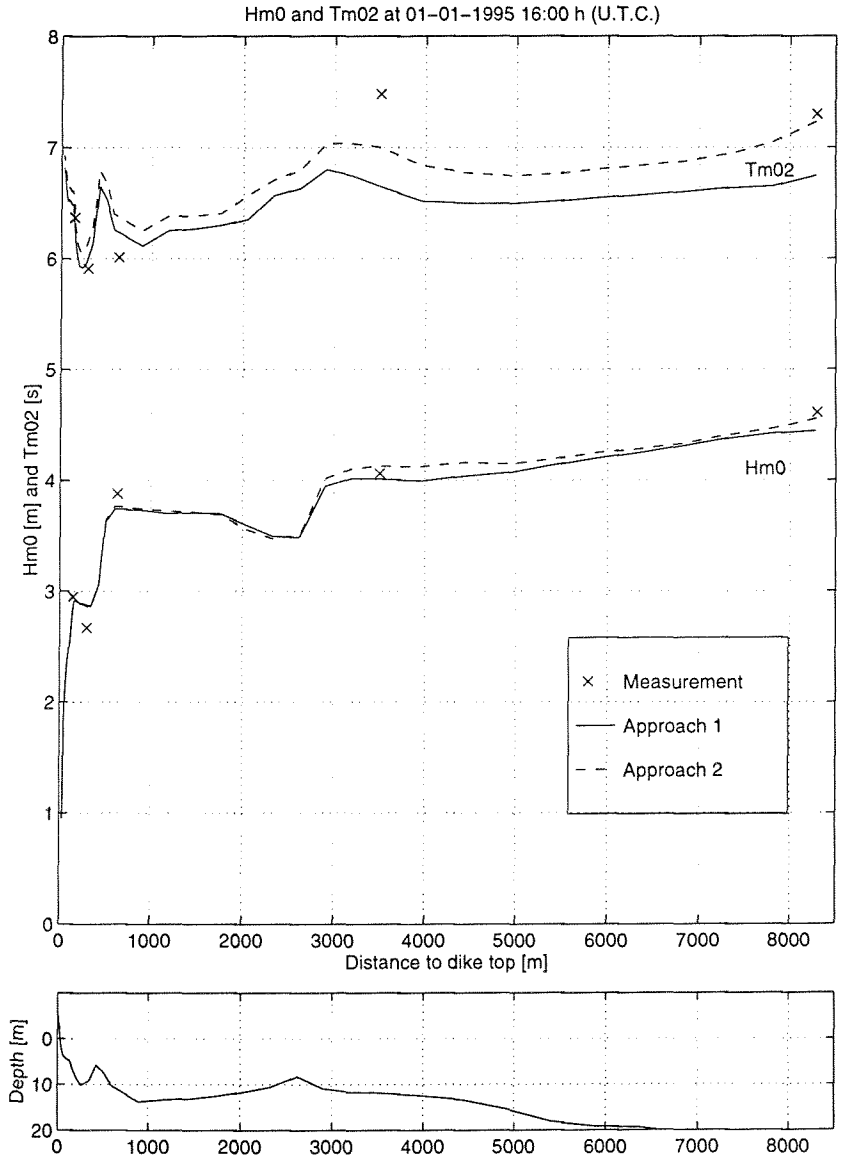

figure 4-4 **Hm_0 and Tm_{02} along the Petten transect at 1-1-1995 16:00 h.**

In figure 4-5 energy density spectra along the Petten transect for approach 2 are presented. The energy density spectra are compared to the observed spectra only for approach 2, because this is the approach with the observed spectrum in station Mp1.

Station Mp1 is the location of the offshore wave boundary condition. In station Mp2 the peak of the energy density estimated by the SWAN computation and the observed peak differs 2.5 m^2/Hz.

In Mp3, located just offshore the bank nearest the dike, the peak energy densities for both the computed and the observed spectra are lower than at Mp2. At Mp3 the energy density at the peak frequency is about the same for the computed and observed spectra. The agreement at Mp3 between the observed and the calculated spectrum for the high frequency side of the spectrum is good. The tail of the observed spectrum fluctuates around the more stable tail of the computed spectrum.

The shape of the spectrum has changed in station Mp5 compared to the shape of the spectrum at station Mp3. The peak energy density is much lower while the energy density above 0.2 Hz decreased only slightly compared to the spectrum in station Mp3.

The peak energy density increases from station Mp5 to Mb6 by 10 %. The peak frequencies do not change in the observations nor in the computations from station Mp5 to Mb6. The energy density in the computation underestimates the observed energy density for the range from 0.15 Hz till 0.3 Hz. Above 0.3 Hz no energy density is assumed present in the observation because of the measuring device, so no comparison can be made for this frequency range.

Overall, the agreement of the observed spectra with the calculated spectra for all stations is fairly good.

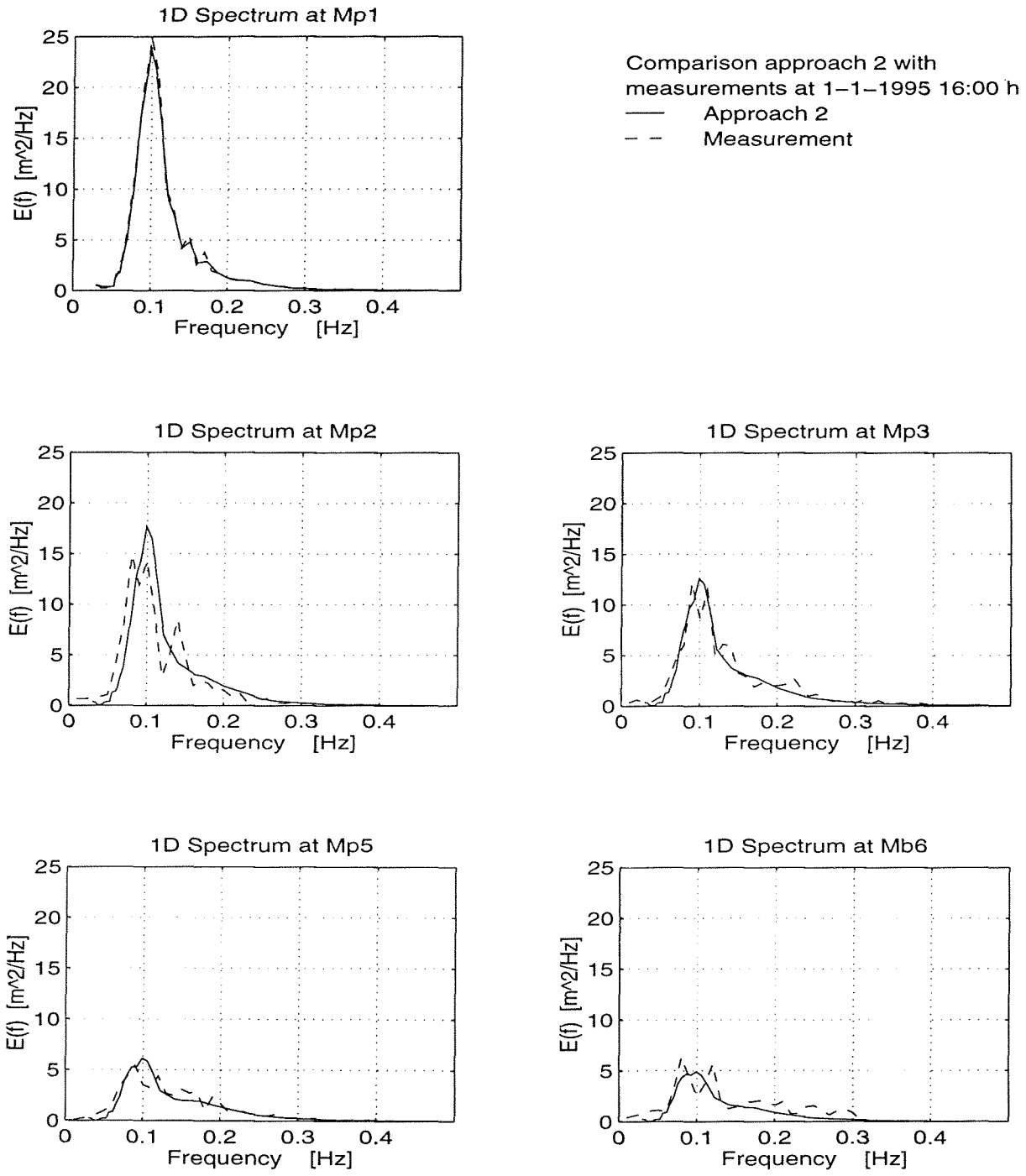

figure 4-5 **1-D spectra along Petten transect at 1-1-1995 16:00 h.**

Case 2: January 2nd 04:00 h(U.T.C.) 1995

Results from computations and the measurements of the 2nd of January 1995 at 04:00 hours are presented in table 4-5, figure 4-6, figure 4-7 and figure 4-8.

	Measurement			Comp. approach 1			Comp. Approach 2 (starting at Mp1)		
Station:	Hm_0 [m]	Tm_{01} [s]	Tm_{02} [s]	Hm_0 [m]	Tm_{01} [s]	Tm_{02} [s]	Hm_0 [m]	Tm_{01} [s]	Tm_{02} [s]
Mp1	5.05	8.81	7.68	5.46	8.98	7.70	4.98	8.75	7.58
Mp2	4.71	9.03	7.98	4.51	8.59	7.44	4.50	8.34	7.25
Mp3	4.04	7.12	5.88	3.97	8.01	6.77	3.96	7.93	6.73
Mp4				3.95	8.02	6.78	3.94	7.94	6.74
Mp5	3.04	7.45	6.43	3.06	7.85	6.62	3.07	7.84	6.66
Mp6	3.11	7.75	6.83	2.79	8.58	7.32	2.79	8.60	7.39

table 4-5 Comparison approach 1 and 2 with measurements

The relative difference in Hm_0 between approach 1 and 2 in this case is 8.8% of the value of approach 2 at station Mp1. This difference near the coast at Mp6 is 0.4%. This decrease between the two approaches towards the coast is visible in figure 4-7.

The relative difference in Tm02 for station Mp1 is small only 1.4% which also can be seen from the shapes of both spectra (figure 4-6) which are roughly the same. The difference in Tm_{02} for station Mp6 nearshore is 0.9% this change in Tm_{02} along the Petten transect is shown in figure 4-7.

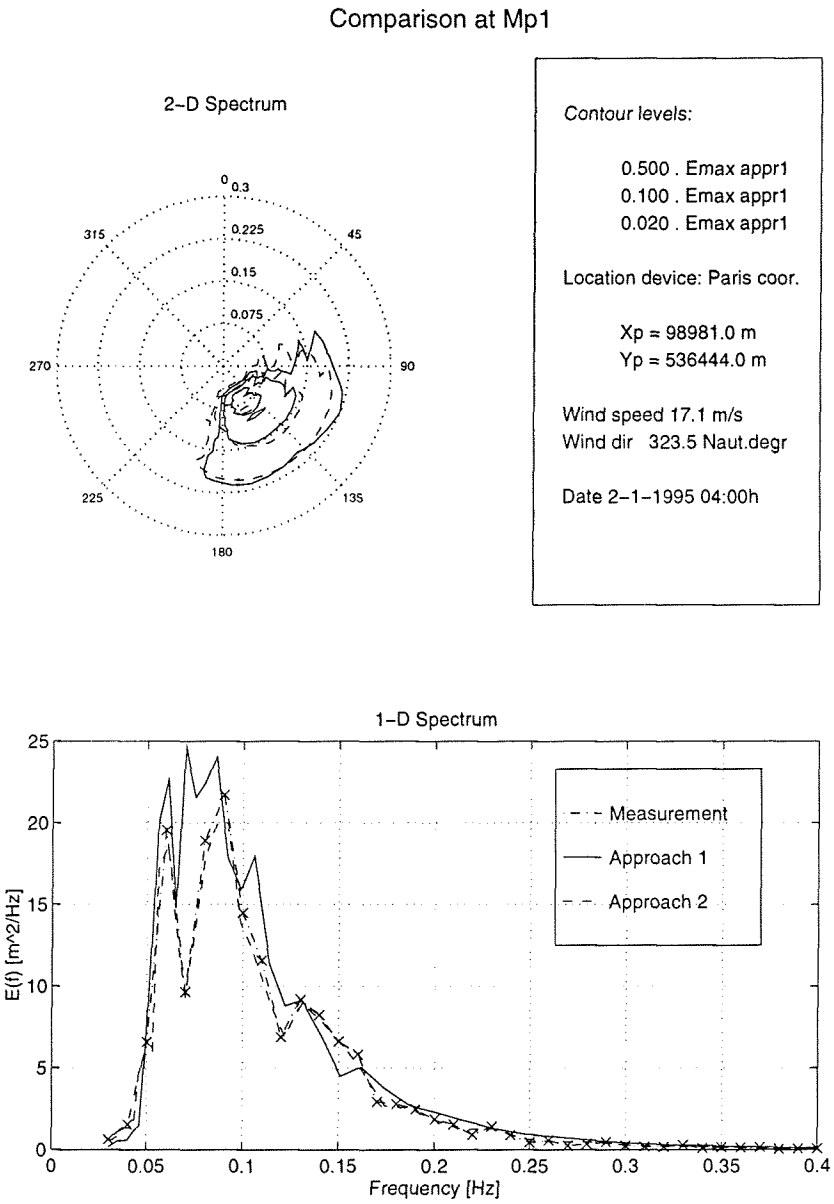

figure 4-6 **Comparison energy density spectra approach 1 and approach 2 with measurement at station Mp1 at 2-1-1995 04:00 h (U.T.C.).**

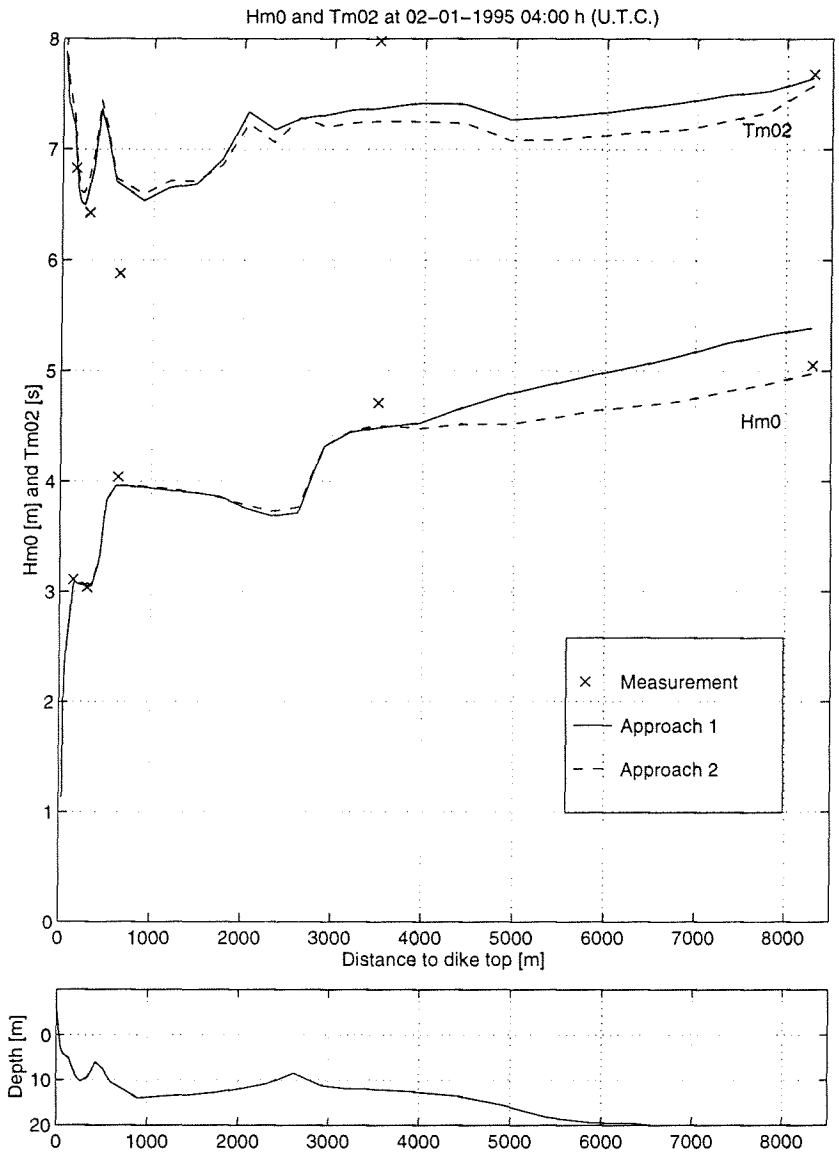

figure 4-7 **Tm_{02} along the Petten transect at 2-1-1995 04:00 h.**

Only the results of approach 2 are compared to the observed spectra.

All calculated spectra agree well with the observed ones (figure 4-8. At station Mp5 there seems to be a peak in the energy spectrum at about 0.15 Hz. This peak is consistently present in the registrations of spectra of station Mp5 around this time, however at this point in time it is extremely high.

The spectrum at station Mp1 is the input spectrum for the model. For the spectrum at station Mp2 the peak frequency in the computations is about 0.02 Hz higher than in the observed spectrum. The calculated energy density above 0.17 Hz is slightly higher than the observed energy density for this station. The energy density at the peak frequency is lower than the observed peak energy level (2.0 m^2/Hz).

The high frequency sides for the spectra in stations Mp3 and Mp5 agree well. The peak energy density in station Mp3 is about equal to the observed one but at a 0.04 Hz lower frequency.

The energy level for station Mb6 is underestimated for the frequencies above 0.2 Hz.

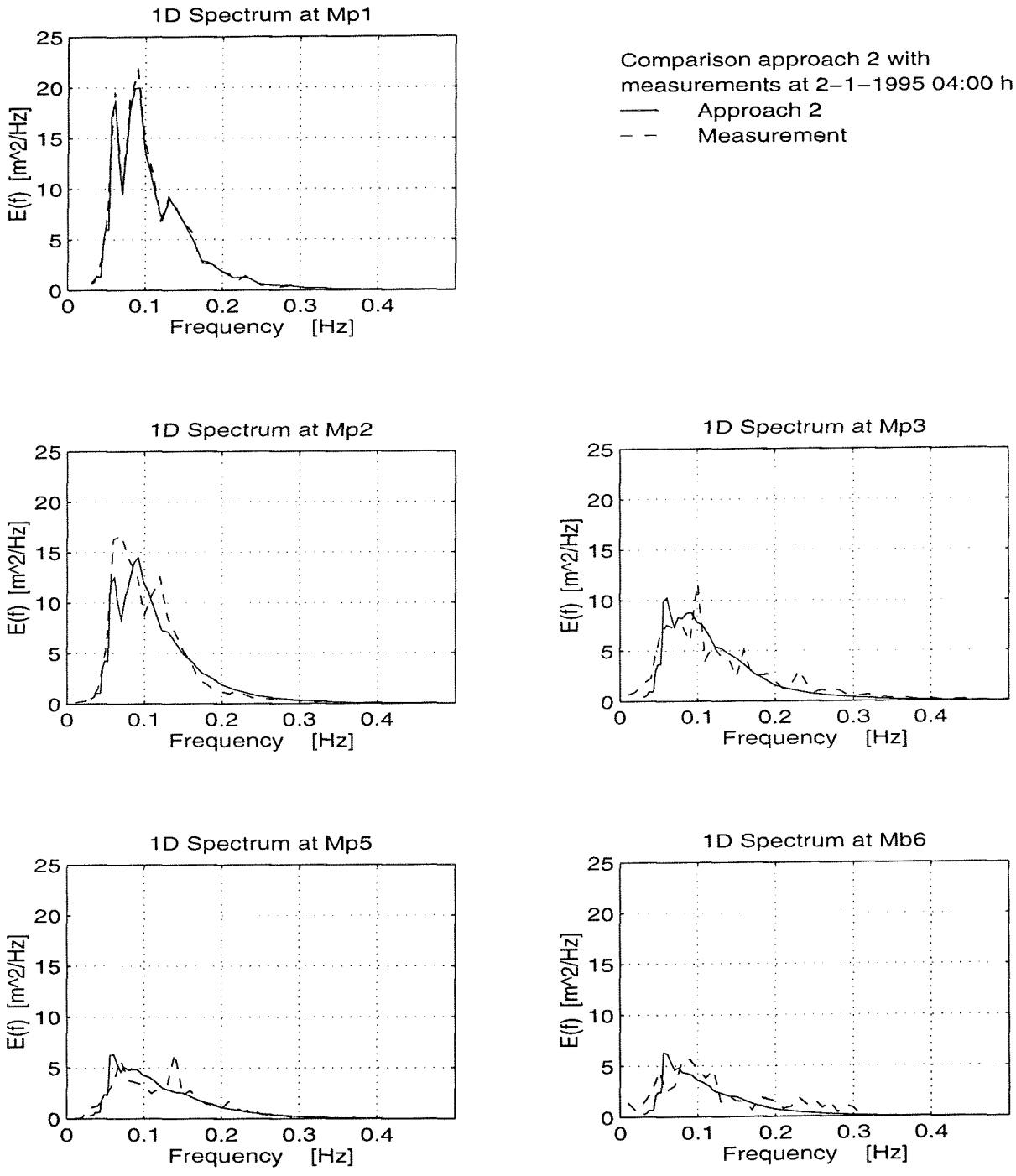

figure 4-8 1-D spectra along Petten transect at 2-1-1995 04:00 h.

Case 3: January 10th 11:00 h (U.T.C.) 1995

Results from computations and the measurements of the 10th of January 1995 are presented in table 4-6, figure 4-9. figure 4-10 and figure 4-11.

	Measurement			Comp. approach 1			Comp. approach 2 (starting at Mp1)		
Station:	Hm_0 [m]	Tm_{01} [s]	Tm_{02} [s]	Hm_0 [m]	Tm_{01} [s]	Tm_{02} [s]	Hm_0 [m]	Tm_{01} [s]	Tm_{02} [s]
Mp1	4.57	8.63	7.73	4.23	7.67	6.70	4.50	8.49	7.44
Mp2	4.02	8.54	7.57	3.82	7.51	6.63	4.06	8.32	7.40
Mp3	3.58	7.05	6.28	3.61	7.22	6.27	3.68	7.70	6.62
Mp4				3.58	7.23	6.29	3.66	7.71	6.63
Mp5	3.16	7.54	6.76	2.84	6.99	6.06	2.89	7.42	6.36
Mp6	2.85	7.10	6.33	2.54	7.52	6.61	2.60	8.02	6.95

table 4-6 Comparison approach 1 and 2 with measurements

At station Mp1 the relative difference between the two approaches in Hm_0 is 6.0% of the value of approach 2. At station Mb6 this difference is 2.3% of approach 2 (figure 4-10). The relative difference in mean period Tm_{02} at the offshore boundary is 9.9% of the value obtained in approach 2. This difference is 4.9% of approach 2 nearshore at Mp6. The change in period along the Petten transect can be seen in figure 4-10.

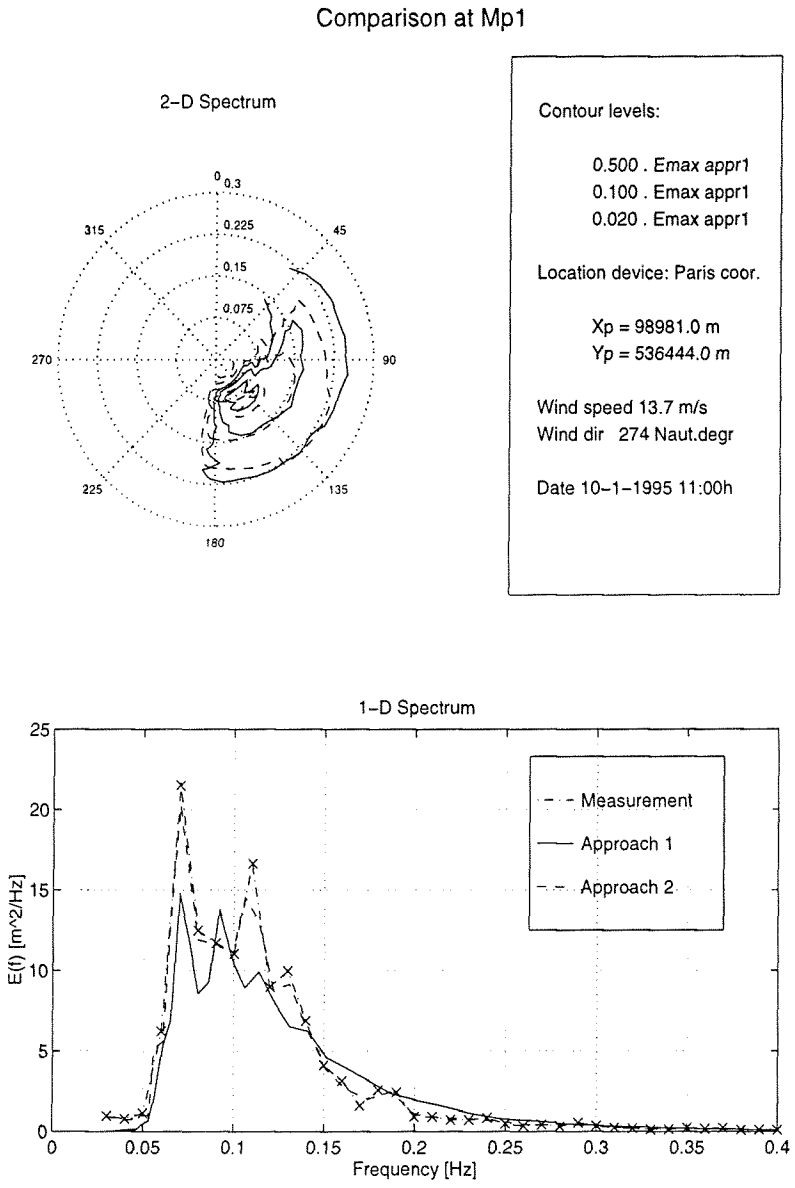

figure 4-9 **Comparison energy density spectra approach 1 and approach 2 with measurement at station Mp1 at 10-1-1995 11:00 h (U.T.C.).**

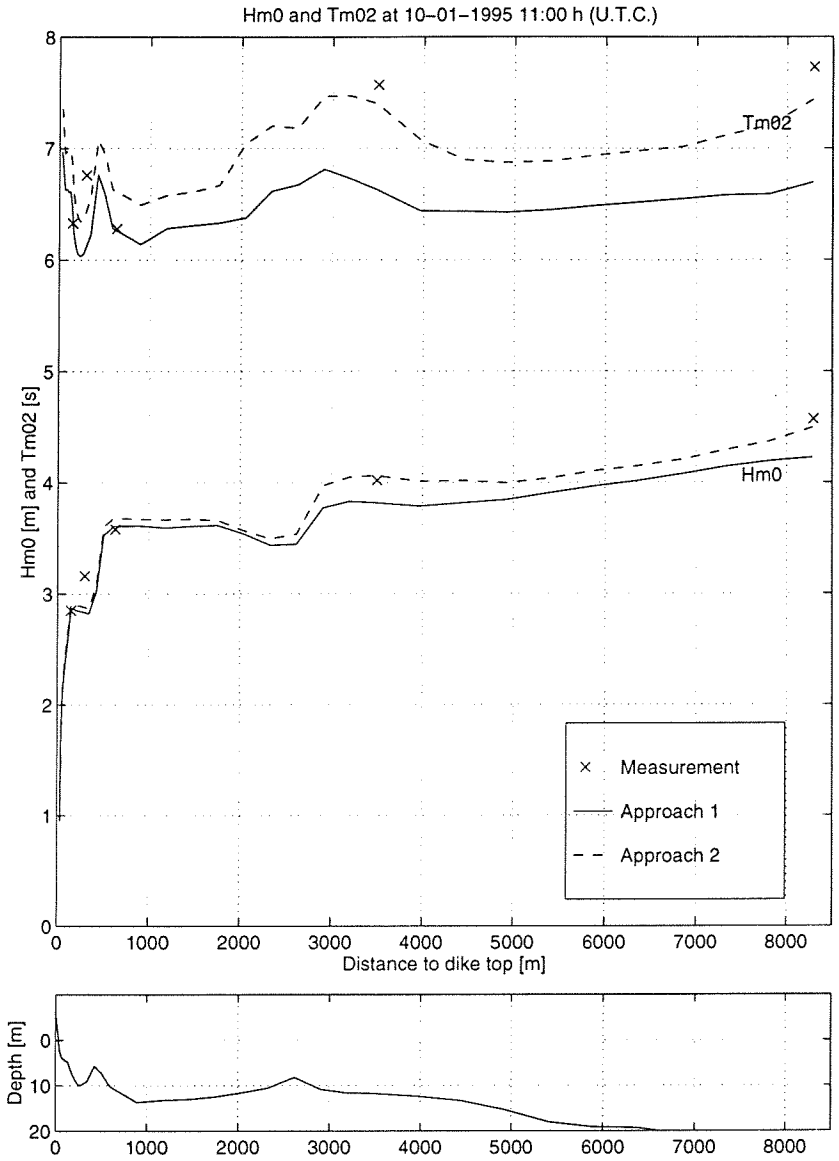

figure 4-10 **Tm_{02} along the Petten transect at 10-1-1995 11:00 h.**

The comparison between the observed and measured spectra is made for approach 2 only.

The calculated energy density spectra agree well with observed spectra (figure 4-11). The spectrum at station Mp1 is the input spectrum. The computed spectrum at station Mp2 resembles the observed spectrum well. The highest energy level has the same magnitude and is located at the same frequency. The secondary peak is only slightly off (0.01 Hz higher) and the high frequency side of the spectrum (above 0.15 Hz) resembles the observed one.

For the computed spectrum at station Mp3 the highest energy level is about equal to that of the observed spectrum but at a lower frequency (0.03 Hz). The energy between 0.17 and 0.20 Hz is underestimated and the energy above 0.20 Hz resembles the observed spectrum well.

For station Mp5 and Mb6 the energy level in the computed spectrum between 0.1 and 0.2 Hz (even higher for Mb6) is underestimated. The peak energy levels are

predicted at a lower frequency than observed. The magnitude of the peak energy level is about right for the energy at station Mb6. In station Mp5 the energy level for the peak frequency is estimated lower than the observed peak energy level.

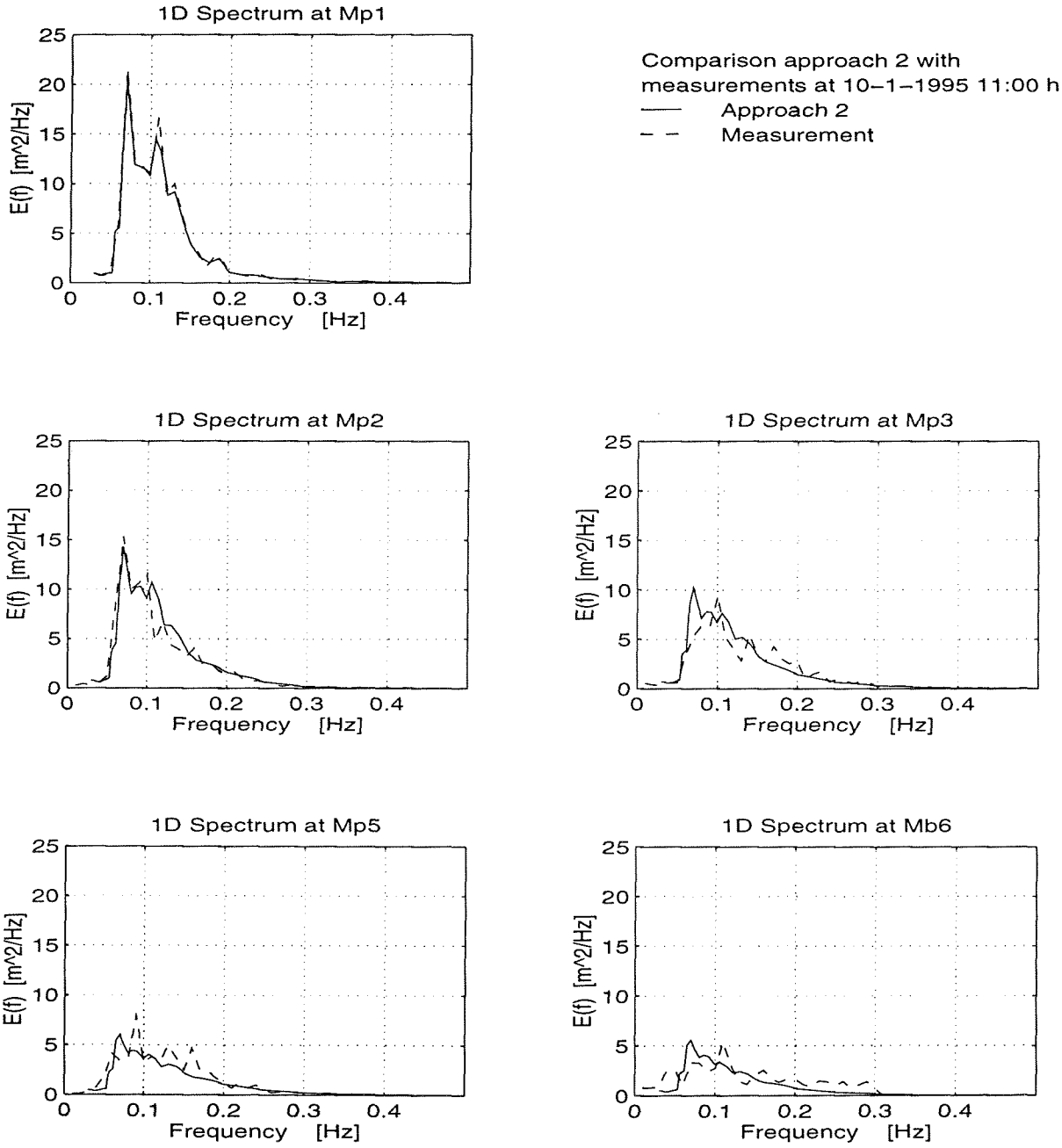

figure 4-11 1-D spectra along Petten transect at 10-1-1995 11:00 h.

4.2.2 Comments

For all three cases the differences between approach 1 and approach 2, for the wave height Hm_0 as well as for the mean wave period Tm_{02} are getting smaller shore ward.

Wave heights at station Mp1 calculated with approach 1 differ less than 10% from the measurements (and approach 2).

In Case 1 the energy density spectrum in station Mp1 differs the most in the two approaches. The spectra in station Mp1 in the other two approaches agree fairly well especially taken the inaccuracies in the measuring devices into account.

Calculated wave heights near the Petten dike for both approaches agree well with each other but there are differences especially in the part offshore of the 'Pettemer Polder'. Shoreward of the 'Pettemer Polder' the local topography is dominant for the wave field so for equal boundary conditions (water-level set-up and wind) the calculated wave heights agree between the two approaches.

Only approach 2 is used because of the accurate offshore boundary condition and not one derived from far away offshore stations.

To quantify the performance of the model three indices are used, these are defined as:

Performance index $= \dfrac{\text{rms(error)}}{\text{rms(observed changes)}}$

Scatter index $= \dfrac{\text{rms(error)}}{\overline{Hm_0}}$

Boundary index $= \dfrac{\text{rms(error)}}{Hm_{0\ \text{incoming}}}$ in which :

rms(error) $= \sqrt{\dfrac{1}{n}\sum_{i=1}^{n}\left(Hm_0(Mp_n(\text{meas.})) - Hm_0(Mp_n(\text{comp}))\right)^2}$

rms(observed changes) $= \sqrt{\dfrac{1}{n}\sum_{i=1}^{n}\left(Hm_0(Mp1(\text{meas.})) - Hm_0(Mp_n(\text{meas.}))\right)^2}$

$\overline{Hm_0}$ = average of computed significant wave heights

$Hm_{0\ \text{incoming}}$ = significant wave height used as boundary condition.

Case 1: 1-1-1995 16:00 (U.T.C.)

The differences for the spectral parameters in the measuring stations for case 1 are presented in table 4-7. This shows that the predictions of the model are close (all but one within 10%) to the parameters from the observed spectrum. The indices for this computation are :

Performance index : 0.83

Scatter index : 0.06

Boundary index : 0.05

Station:	$\lvert Hm_0 \rvert$ [m]	Hm_0 [%]	$\lvert Tm_{01} \rvert$ [s]	Tm_{01} [%]	$\lvert Tm_{02} \rvert$ [s]	Tm_{02} [%]
Mp1	0.06	1.3	0.05	0.6	0.07	1.0
Mp2	0.07	1.7	0.56	6.7	0.48	6.4
Mp3	0.11	2.8	0.37	5.3	0.38	6.3
Mp5	0.21	7.8	0.14	2.0	0.18	3.0
Mp6	0.40	13.5	0.44	6.2	0.23	3.6

table 4-7 Differences between measured and simulated values (approach 2 absolute and relative)

Case 2: 2-1-1995 04:00 (U.T.C.)

The differences for the spectral parameters in the measuring stations for case 2 are presented in table 4-8. This shows that the predictions of the model are close (all but two within 10%) to the parameters from the observed spectrum. The indices for this computation are :

Performance index : 0.87

Scatter index : 0.05

Boundary index : 0.04

Station:	$\lvert Hm_0 \rvert$ [m]`	Hm_0 [%]	$\lvert Tm_{01} \rvert$ [s]	Tm_{01} [%]	$\lvert Tm_{02} \rvert$ [s]	Tm_{02} [%]
Mp1	0.07	1.4	0.06	0.7	0.10	1.3
Mp2	0.21	4.5	0.69	7.6	0.73	9.1
Mp3	0.08	1.9	0.81	11.4	0.85	14.5
Mp5	0.03	1.0	0.39	5.2	0.23	3.6
Mp6	0.32	10.3	0.85	11.0	0.56	8.2

table 4-8 Differences between measured and simulated values (approach 2 absolute and relative)

Case 3: 10-1-1995 11:00 (U.T.C.)

The differences for the spectral parameters in the measuring stations for case 3 are presented in table 4-9. This shows that the predictions of the model are close (all but one within 10%) to the parameters from the observed spectrum. The indices for this computation are :

Performance index : 0.84

Scatter index : 0.06

Boundary index : 0.04

Station:	$\|Hm_0\|$ [m]	Hm_0 [%]	$\|Tm_{01}\|$ [s]	Tm_{01} [%]	$\|Tm_{02}\|$ [s]	Tm_{02} [%]
Mp1	0.07	1.5	0.14	1.6	0.29	3.8
Mp2	0.04	1.0	0.22	2.6	0.17	2.2
Mp3	0.10	2.8	0.65	9.2	0.34	5.4
Mp5	0.27	8.5	0.12	1.6	0.40	5.9
Mp6	0.25	8.8	0.92	12.9	0.62	9.8

table 4-9 Differences between measured and simulated values (approach 2 absolute and relative)

5 Sensitivity

5.1 General

The sensitivity of the computed results to changes in the input parameters has been investigated. It is necessary to choose the parameters with great care and for which parameters the accuracy is less critical. This knowledge is needed to understand the influence of each parameter on the results and to calibrate the model for this area. The sensitivity study is performed for one case (Case 2 approach 2, Chapter 4). This case is chosen because of the highest the performance index, (best accordance with measurements).

The sensitivity is determined for variations in:

- Numerics.
- Boundary conditions.
- Physics.

5.2 Sensitivity to numerics

The sensitivity to variations in numerical parameters is presented in this paragraph.

For a description of area 2 and area 3 see section 4.1.2

	Number of meshes [X x Y]	Mesh size	Number of meshes [MDC]
A1	200 x 200 area 2 100 x100 area 3	62.5m x 100m area 2 10m x 20m area 3	32 = 9°
N1	100 x 100 area 2 50 x 50 area 3	125m x 200m area 2 20m x 40m area 3	
N2		62.5m x 100m area 2 10m x 20m area 3	16 = 18°

table 5-1 Changed numerical values in sensitivity

N1 = resolution in x,y space doubled.
N2 = resolution in θ space doubled.

N1 Double resolution in x-y space

The consequence of doubling the resolution in x-y space is that not all variations in bottom profile are 'seen' or exaggerated. This can result in greater wave heights shoreward the bank, because the most shallow part of the bank is not 'seen' in the case with the lower resolution so less energy dissipates which results in a higher significant wave shoreward the bank, this can be seen in figure 5-1 between 3000m and 2000m offshore.

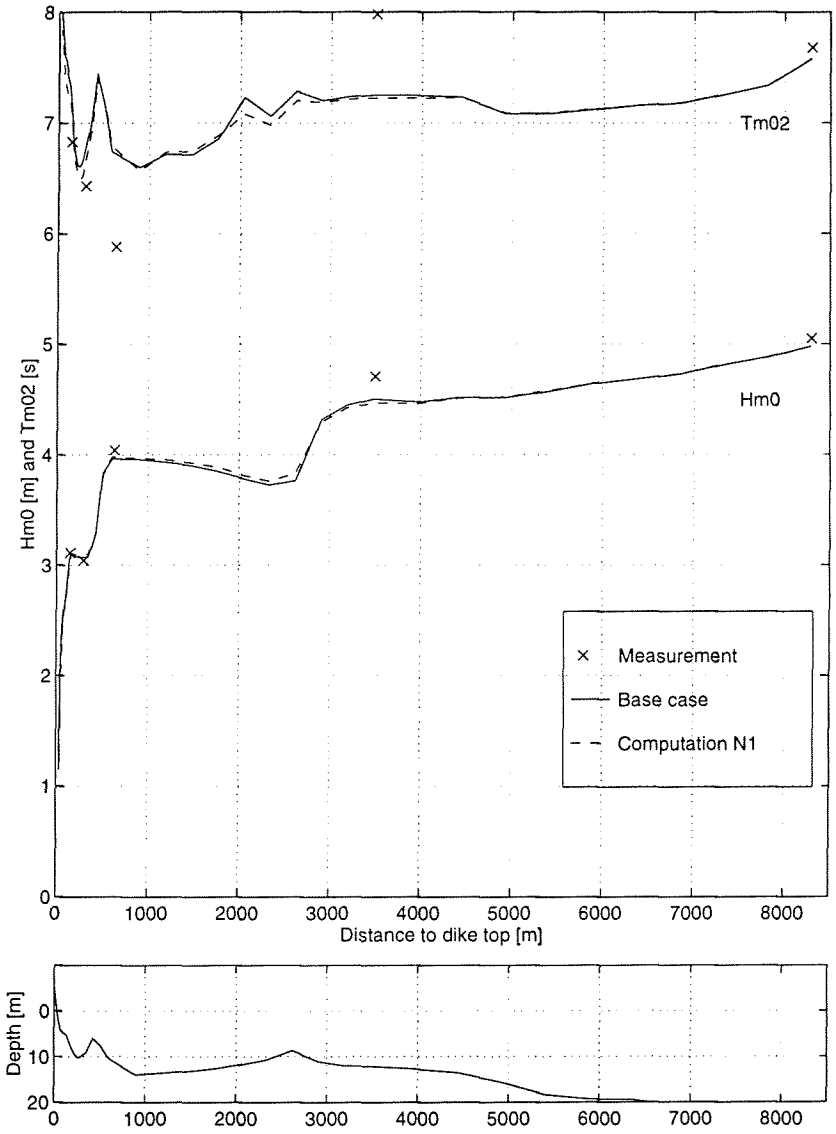

figure 5-1 **Hm_0 and Tm_{02} along the Petten transect for case N1**

N2 **Double the resolution in directional space.**

The differences in Hm_0 are mainly from 7000 m to 4000 m offshore. The differences between the base case and run N2 for periods are mainly in the region between 2500 m and 1000 m offshore (figure 5-2).

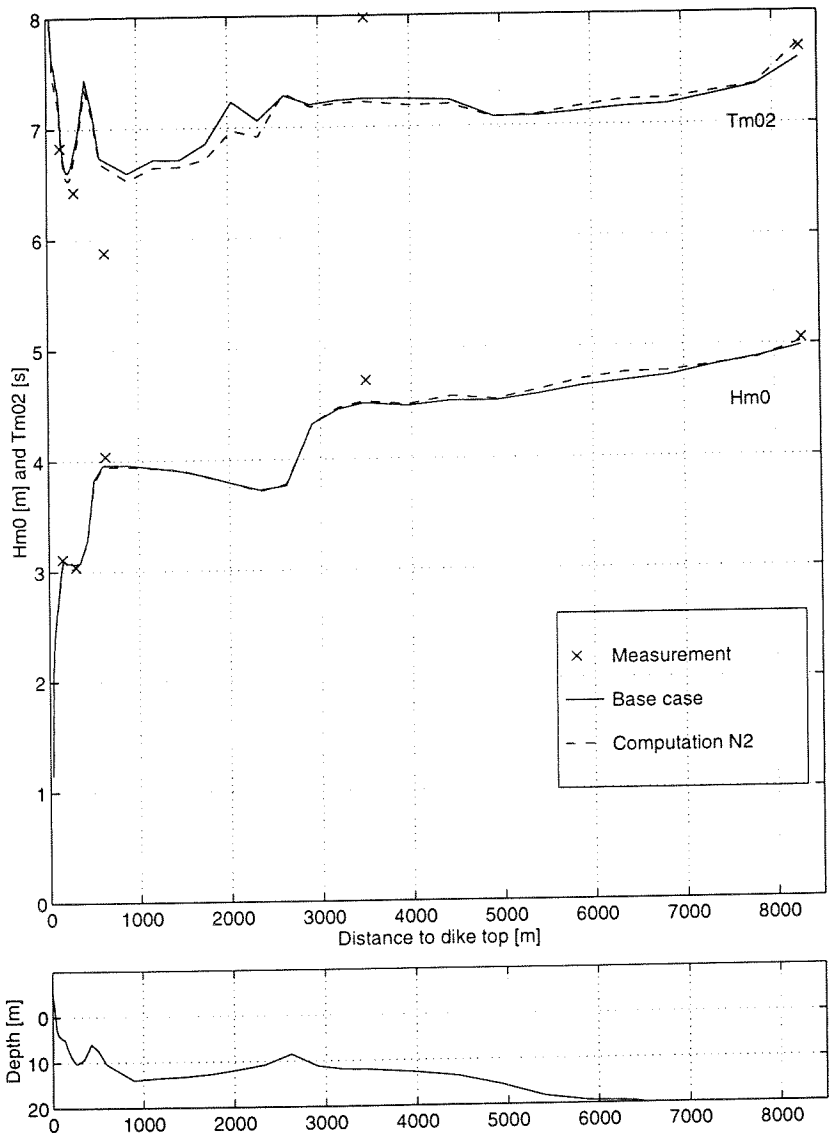

figure 5-2 **Hm_0 and Tm_{02} along the Petten transect for case N2**

5.3 Sensitivity to variation in boundary conditions

The sensitivity to variation in boundary conditions is looked at to investigate to which input boundary condition special care must be taken and which boundary condition can be looked at less critically. The changes are made to the offshore wave boundary condition by numerically altering the energy density of the input spectrum from station Mp1 (table 5-2).

For case A2 the waterlevel is increased by 0.20 m

For case A3 the energy density is shifted over the frequencies so that the peak frequency is equal to 1/12 s^{-1} (i.e. 0.083 Hz).

For case A4 the wind speed is increased by 0.5 m/s.

For case AA the energy density for all frequencies is enlarged with a factor so that the wave height calculated from this spectrum equals 5.10 m.

For case AB three consecutive 20 minutes spectra are averaged in energy density, direction and directional spreading.

	Water level [m]	Peak period [s]	Wind speed [m/s]	Incoming wave Hm_0 [m]
A1	2.20	11.1	17.5	5.05
A2	2.40			
A3		12.0		
A4			18.0	
AA				5.10
AB				5.25 (60 min spectrum)

table 5-2 Changed boundary conditions in sensitivity study

A2 Increased water level with 0.20 meter.

An increase of 0.20 meter in water level leads to increases in wave height. Because the maximum wave height is limited over the breaker bank by the water depth a greater depth leads to a greater wave height. This can be seen in figure 5-3. An overall water level increase of 0.20 meter leads to an increased Hm_0 near the dike of 0.09 meter (3% at station Mp6 nearshore). At station Mp5 (300 m offshore) this is also 0.09 meter. The increase in Hm_0 for station Mp2 in front of the first breaker bank (3500m offshore) is 0.04 meter. The difference in the zero crossing period increases after the breaker banks. Due to a greater depth over these breaker banks less energy is dissipated and the waves that are able to pass the breaker bank have a longer mean zero crossing period.

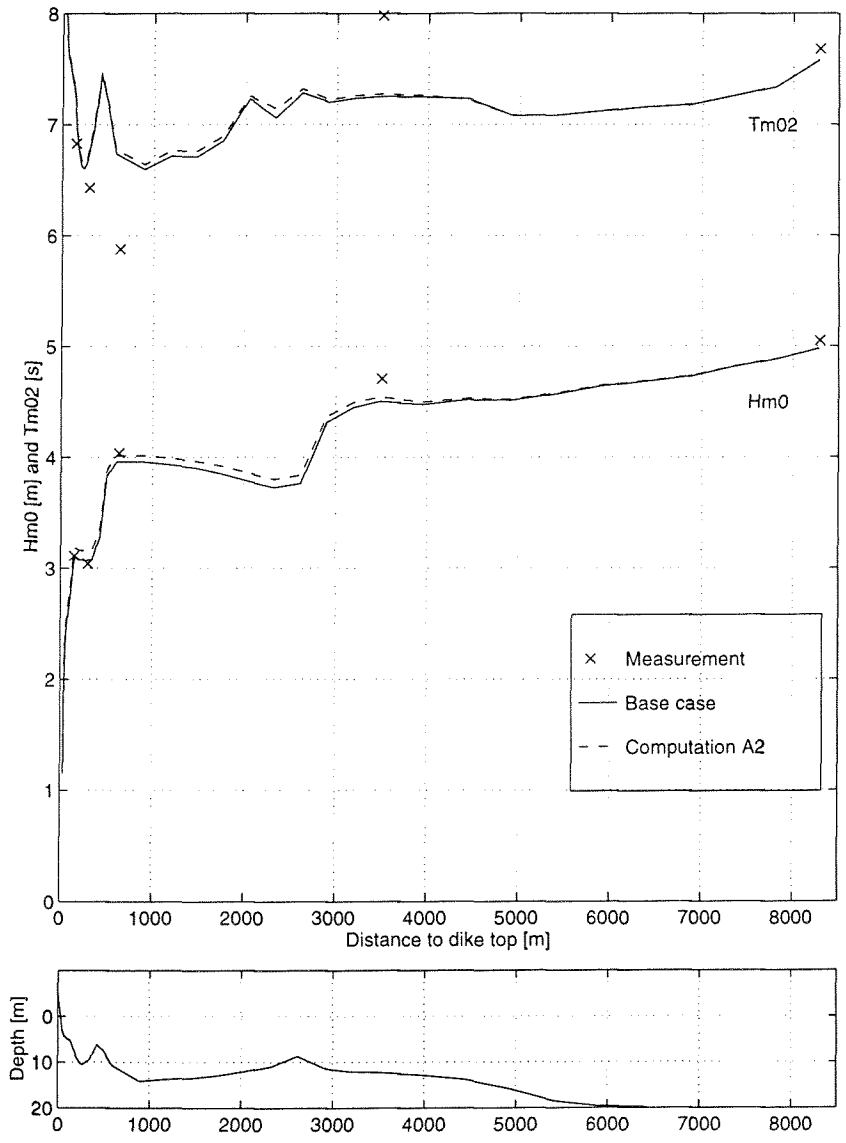

figure 5-3 Hm_0 and Tm_{02} along the Petten transect for case A2

A3 Peak period at a lower frequency (longer period, T_p 12.0 [s]).

The peak period at a lower frequency gives a higher mean period (the new input spectrum has the same shape as the one in the base case but is shifted in frequency). At Mp6 an increase in wave height of 0.04 m compared to the base case is calculated (figure 5-4). The difference, between the mean wave periods for the base case and case A3 is fairly constant from station Mp2 (3500m offshore) until station Mp6 (nearshore) and is about 0.2 seconds.

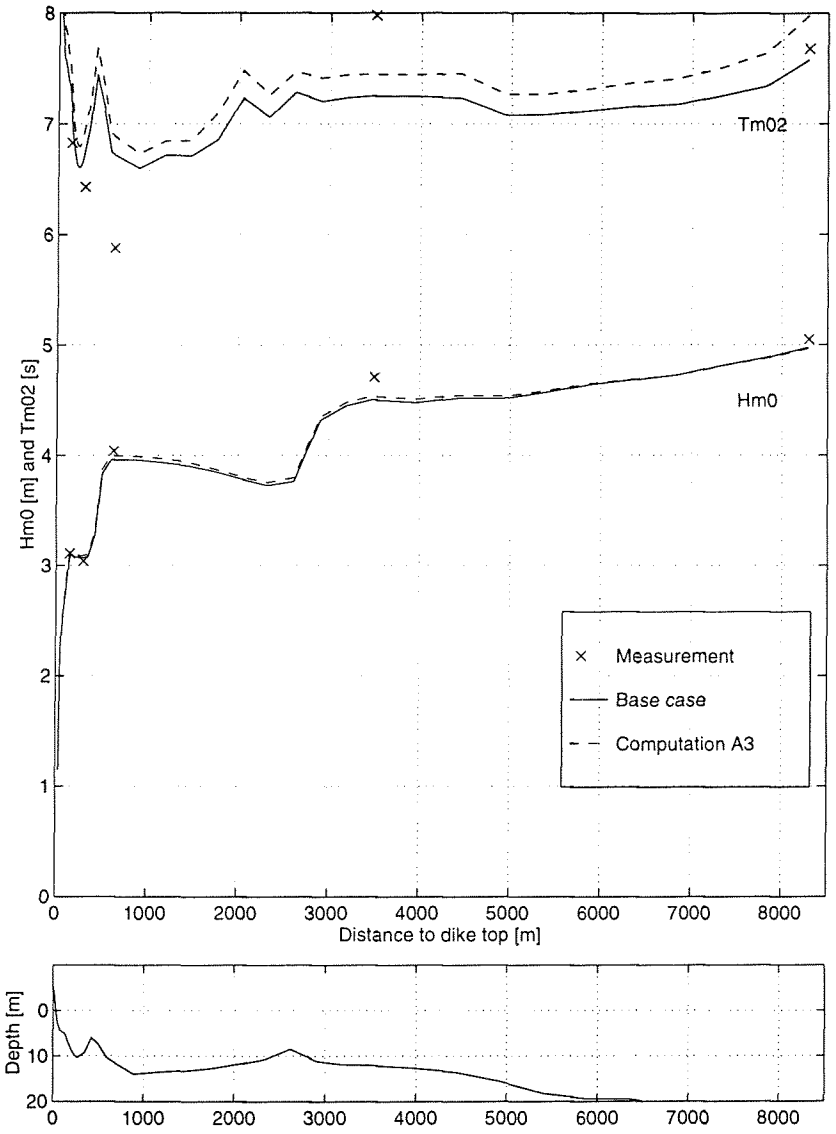

figure 5-4 **Hm_0 and Tm_{02} along the Petten transect for case A3**

A4 Increased wind speed (18.0 [m/s]).

A small increase in windspeed accounts for more growth in the wave height which should result in a slightly higher calculated significant wave height (figure 5-5). In this case the wave height over both breaker banks was limited by the local bottom topography and waterlevel. Shoreward of the breaker banks at 500 meter and 2700 meter offshore the differences with the base case are minimal (less than 2%). The changes in the mean wave periods, compared to the base case, are in the same places. The energy growth due to wind input starts at the high frequency side of the spectrum. Even small increases in energy density in the high frequencies can be seen in changes in mean wave period and even better in the mean zero crossing period (because of the frequency square in the definition).

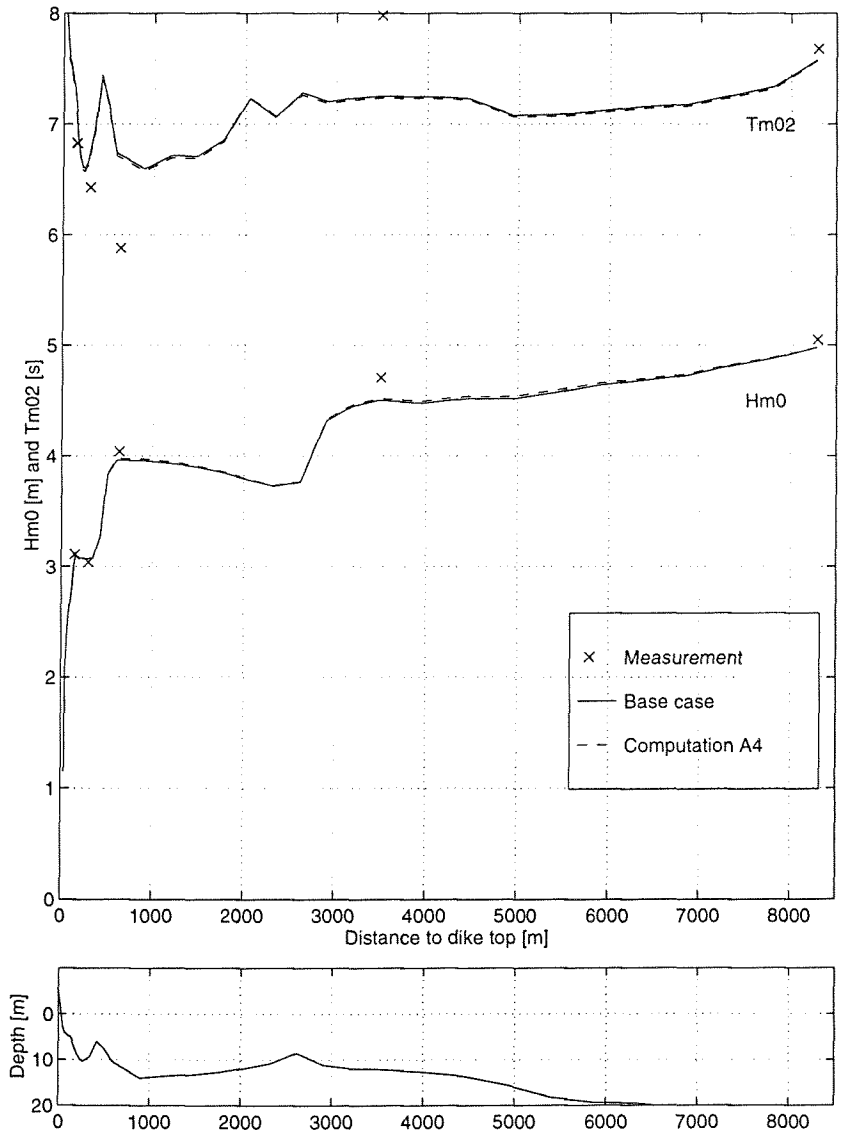

figure 5-5 Hm_0 and Tm_{02} along the Petten transect for case A4

Aa Increased incoming wave height (5.10 [m])

Provided the incoming waves are high enough, the input wave height at the offshore boundary does not have a great impact on the wave height near the dike. The breaker bank has a limiting effect on the wave height in this situation. Shoreward of both breaker banks no effect of the higher incoming wave field is visible (only 0.004 meter left of 0.078 meter increase).

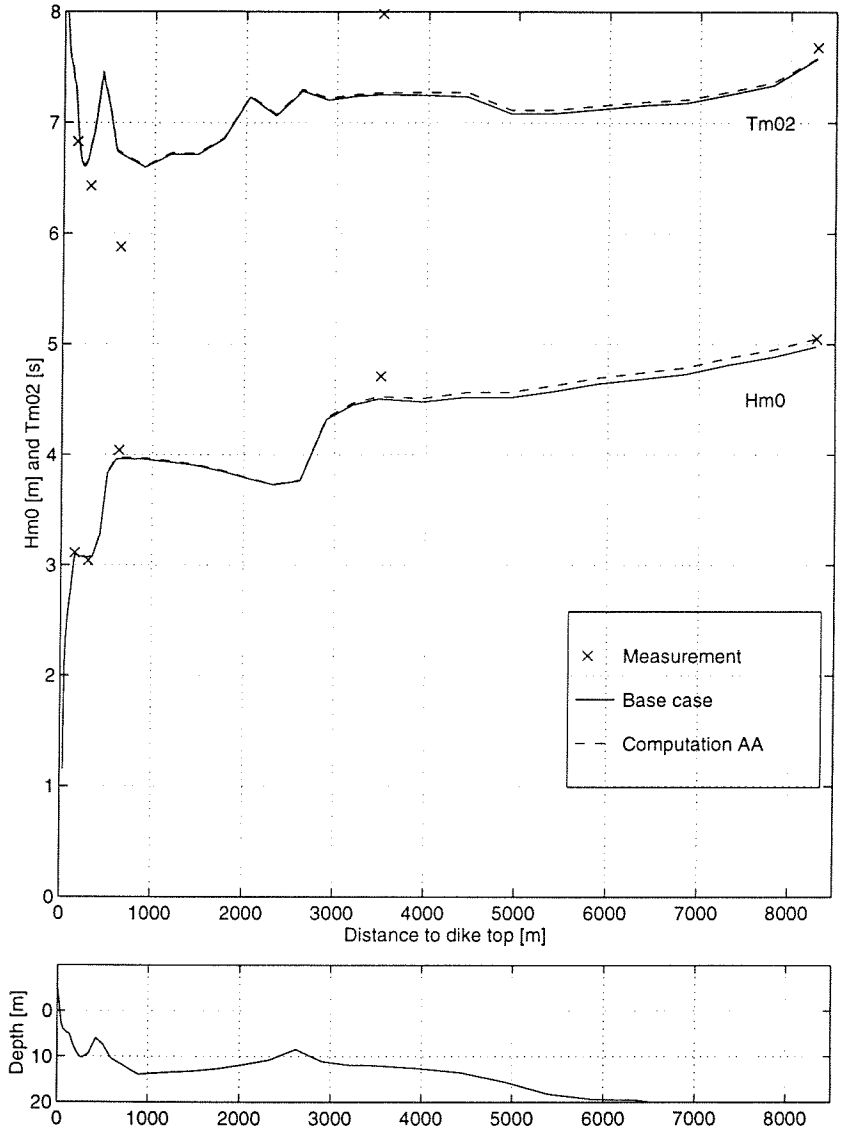

figure 5-6 **Hm_0 and Tm_{02} along the Petten for case Aa**

Ab 60 minutes averaged spectrum.

In three '20 minutes average spectra' computations are compared to one '60 minutes average spectrum' computation. The boundary condition for the '60 minute average spectrum' computation is taken from the average of the three consecutive '20 minute average spectra' covered in this 60 minutes. The idea is to eliminate some inaccuracies in the estimation of the spectral energy density. In figure 5-8 the energy density spectra along the Petten transect are presented. The offshore spectrum in station Mp1 is a 1 peaked spectrum which has no secondary peaks. For the spectrum in station Mp2 more energy dissipated than should be dissipated according the measurements (some 5 m^2/Hz higher peak density). The calculated energy density above 0.17 Hz is higher than in the observed spectrum.

In station Mp3 the energy density peak of the computations is about equal to that of the peak in the observed spectrum but it is at a 0.03 Hz higher frequency of 0.10 Hz. The energy density above 0.17 Hz for this station is underestimated.

In Station Mp5 the energy peak of the spectrum is higher but at the same frequency as the observations. The high frequency side of the energy density spectrum agrees well.

The energy density between 0.2 and 0.3 Hz is underestimated in station Mp6.

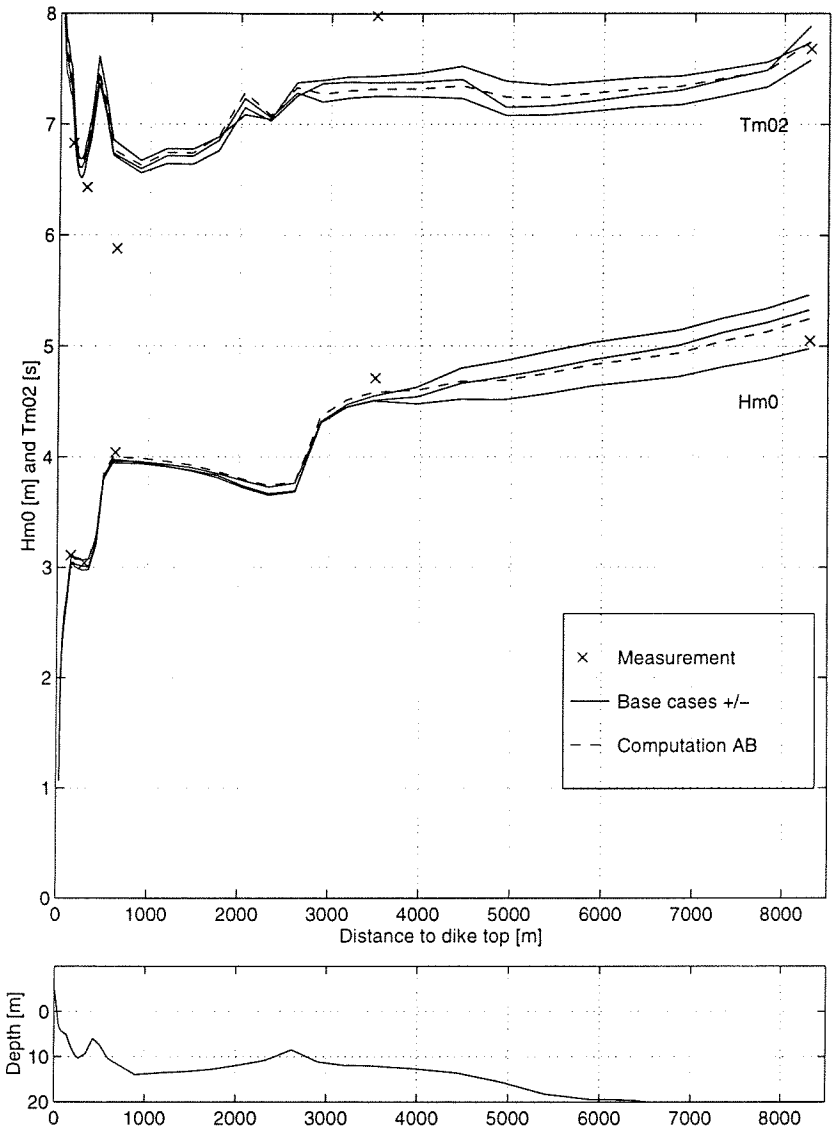

figure 5-7 **Hm_0 and Tm_{02} along the Petten transect for case Ab**

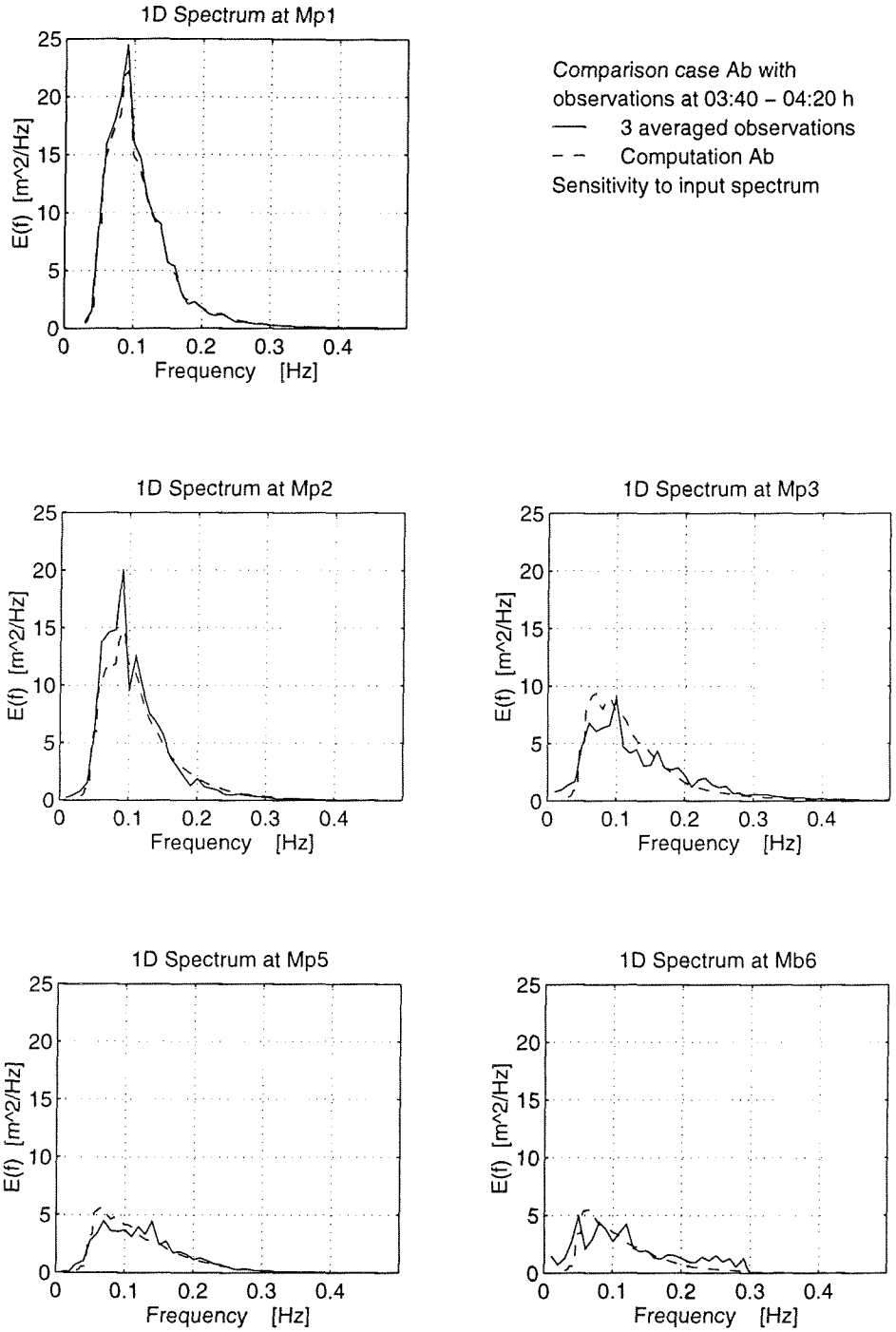

figure 5-8 **60 minute averaged spectra along the Petten transect for case Ab compared with measurements (60 min averaged spectra).**

The 60 min averaged spectra are calculated from three consecutive 20 min spectra from 3:40 till 4:20 h U.T.C.

5.4 Sensitivity to modeled physical processes

The sensitivity to modeled physical processes is presented in this section. The settings for the 2nd and 3rd generation mode in SWAN are presented in table 2-1.

	Bottom friction	Breaker index γ	Triads	Wind formulation
A1	on	0.73	on	Gen 3 Komen
A5	off			
A6		0.65		
A8			off	
A9				Gen 2
AC				Gen 3 Janssen
AD			increased Triad interaction	

table 5-3 Changed parameters in study sensitivity to physics

A5 Bottom friction turned off

The bottom friction is completely turned off in this case. The significant wave height is larger than the wave height calculated in the base case (figure 5-9). This is because no energy is dissipated due to bottom friction. Wave components with low frequencies are more sensitive to friction than high frequency ones, so switching off bottom friction results in higher spectral mean wave periods. The accordance of the calculated wave heights with the measured is better for Mp2 (3500 m) and Mb6 (130 m).

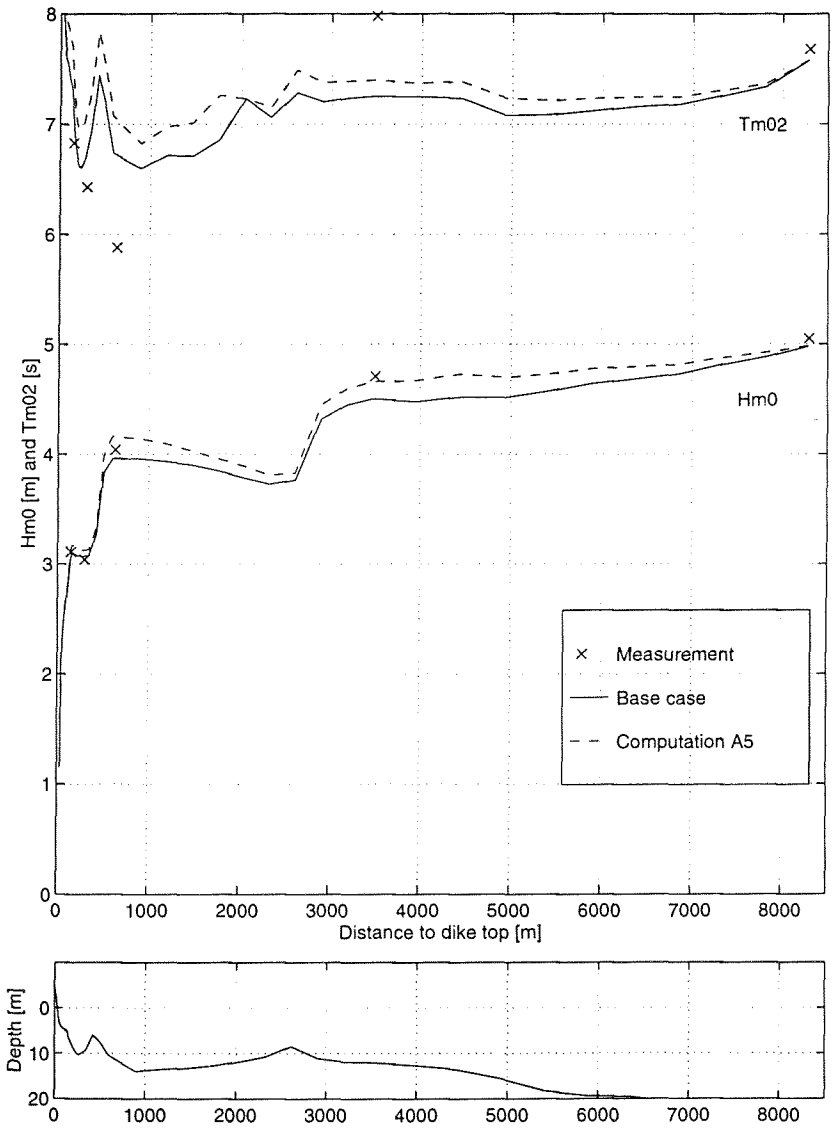

figure 5-9 **Hm_0 and Tm_{02} along the Petten transect for case A5**

A6 Breaker coefficient set to 0.65

The breaker coefficient is set to a lower value so that more energy is dissipated due to depth induced breaking (figure 5-10). The influence of this shows especially round the first breaker bank. The original value of γ (0.73) gives better results than $\gamma = 0.65$, compared with the measurements.

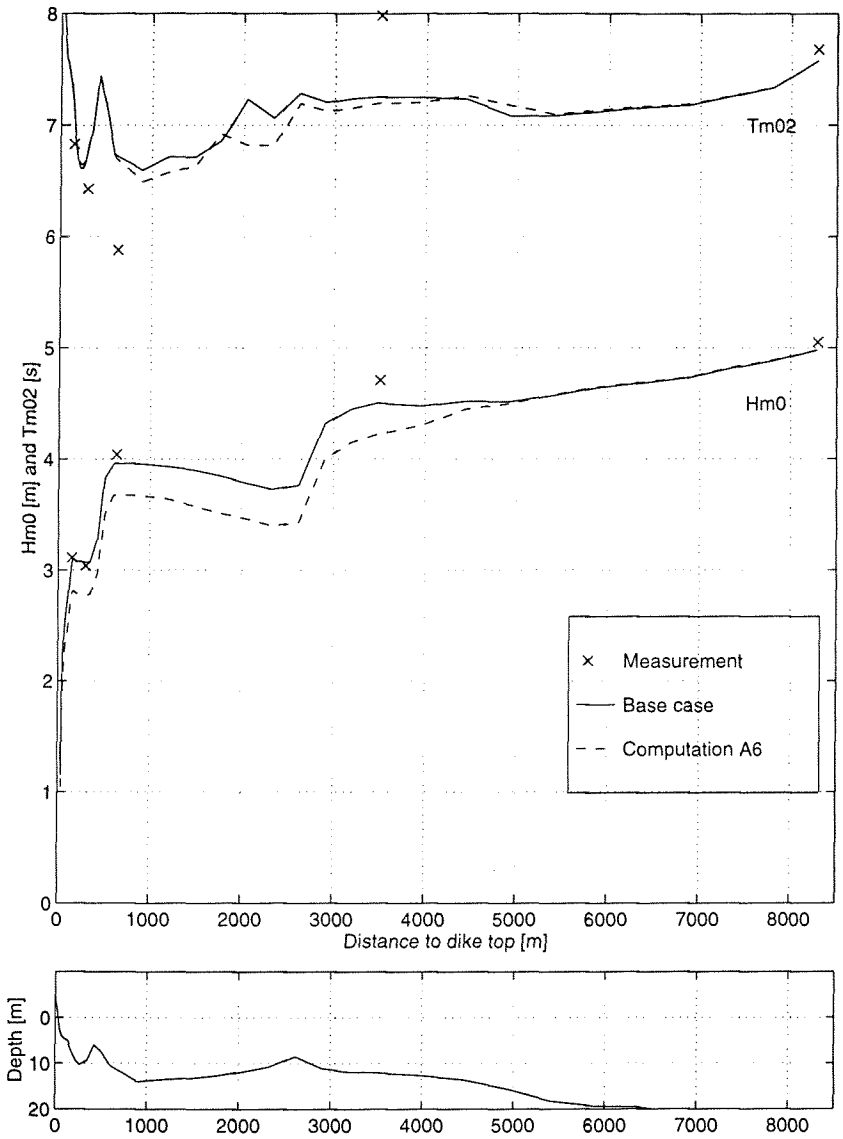

figure 5-10 **Hm_0 and Tm_{02} along the Petten transect for case A6**

A8 Triad interaction turned off

In this case the triad-wave interaction is switched off. The results are presented in figure 5-11 and figure 5-12. It can be seen that, compared to the base case (with triad interaction) the energy density for the peak frequency is higher for the case with the triad interaction switched off and the energy density above 0.13 Hz is lower with the triad interaction switched off. This is expected because no energy redistribution takes place from low to higher frequencies. In the mean period Tm_{02} it is seen that relatively more energy is present for the frequencies between 0.05 Hz and 0.12 Hz for stations near shore (Mp3, Mp5 and Mb6), resulting in higher mean periods.

Further it can be seen that the spectra in the case with the triad interaction have a better match with the observed spectra (figure 5-13). Especially the energy density at the peak frequency is overestimated by case A8. The energy at the high frequency side of the spectrum seems to be underestimated.

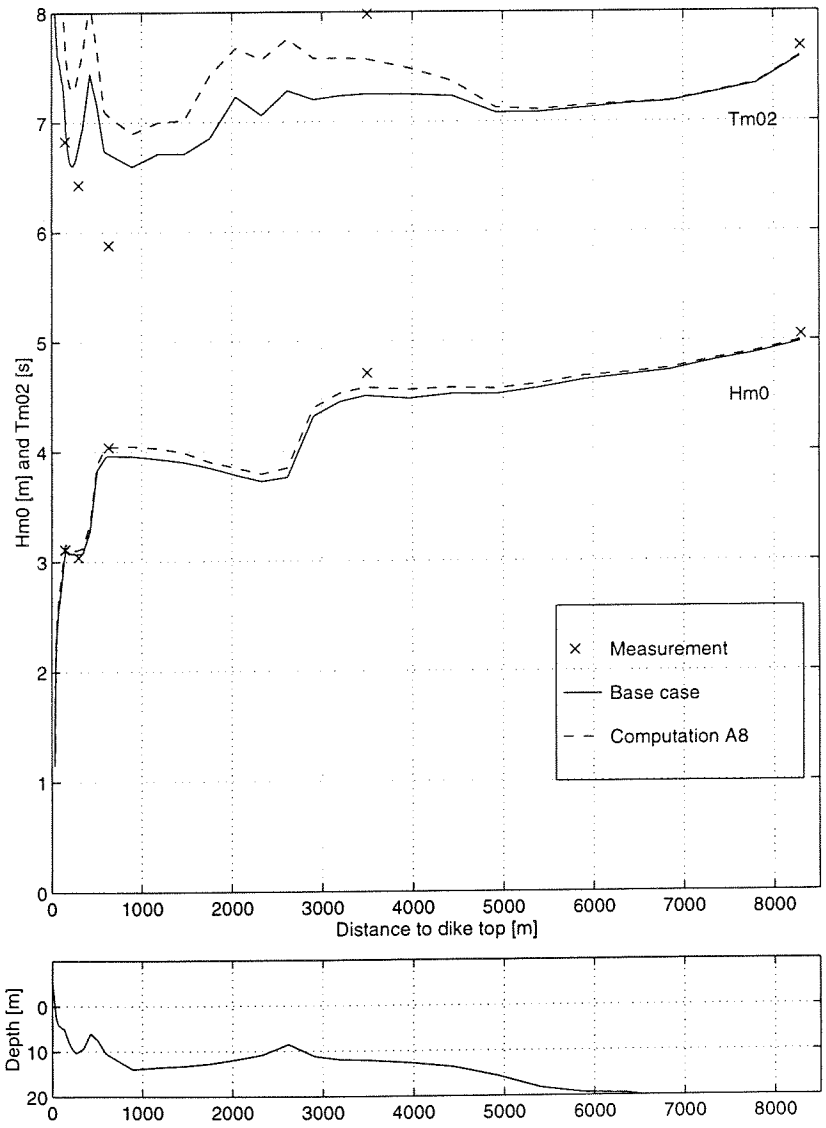

figure 5-11 **Hm_0 and Tm_{02} along the Petten transect for case A8**

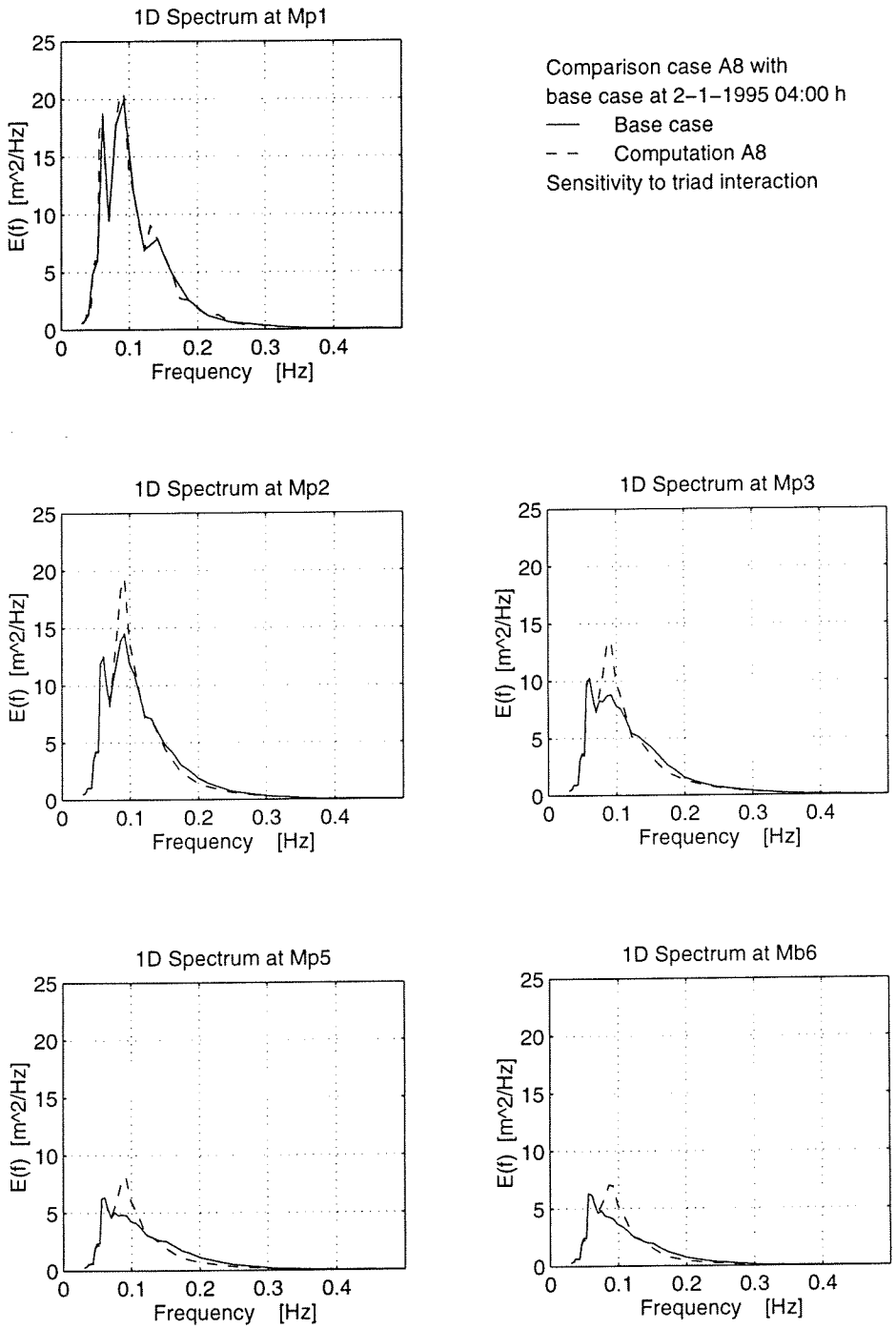

figure 5-12 Spectra along Petten transect for case A8

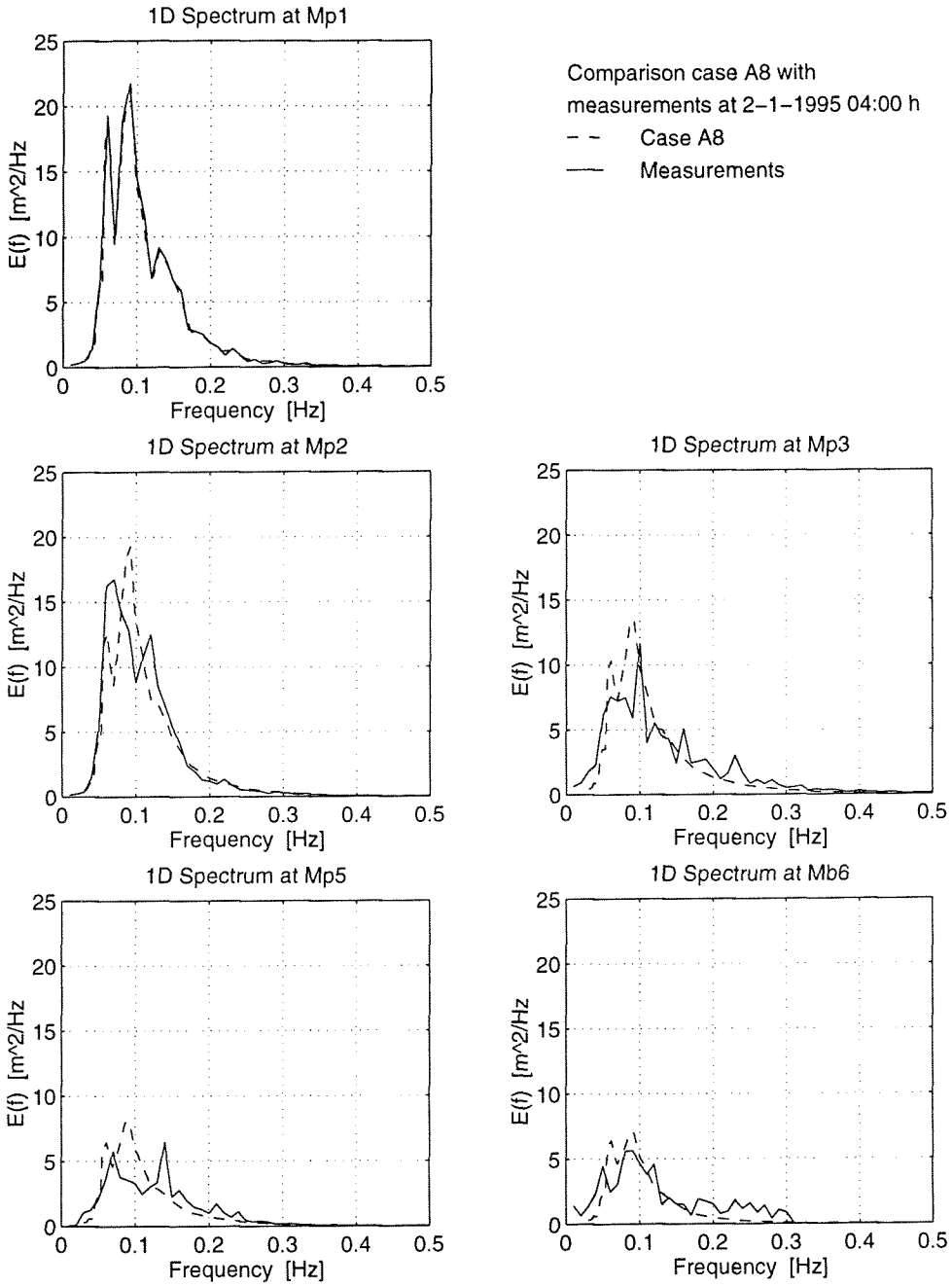

figure 5-13 Spectra along Petten transect for case A8

Ad Triad interaction made 5 times stronger.

In this case the triad-wave interaction is made five times stronger than the base case to see the effect of the triad interaction on the spectrum (figure 5-14) and figure 5-15). The energy density on the high frequency side of the spectrum increases slightly but the energy density of the peak frequency decreases strongly. So, the slight increase needed for a better match with the observations at the high frequency side of the spectrum results in a large unwanted decrease near the peak frequency. The energy gain in the high frequencies is diminished by the dissipation that takes place in this zone. Compared to the observation (figure 5-16) the energy density for the peak frequency now is too low.

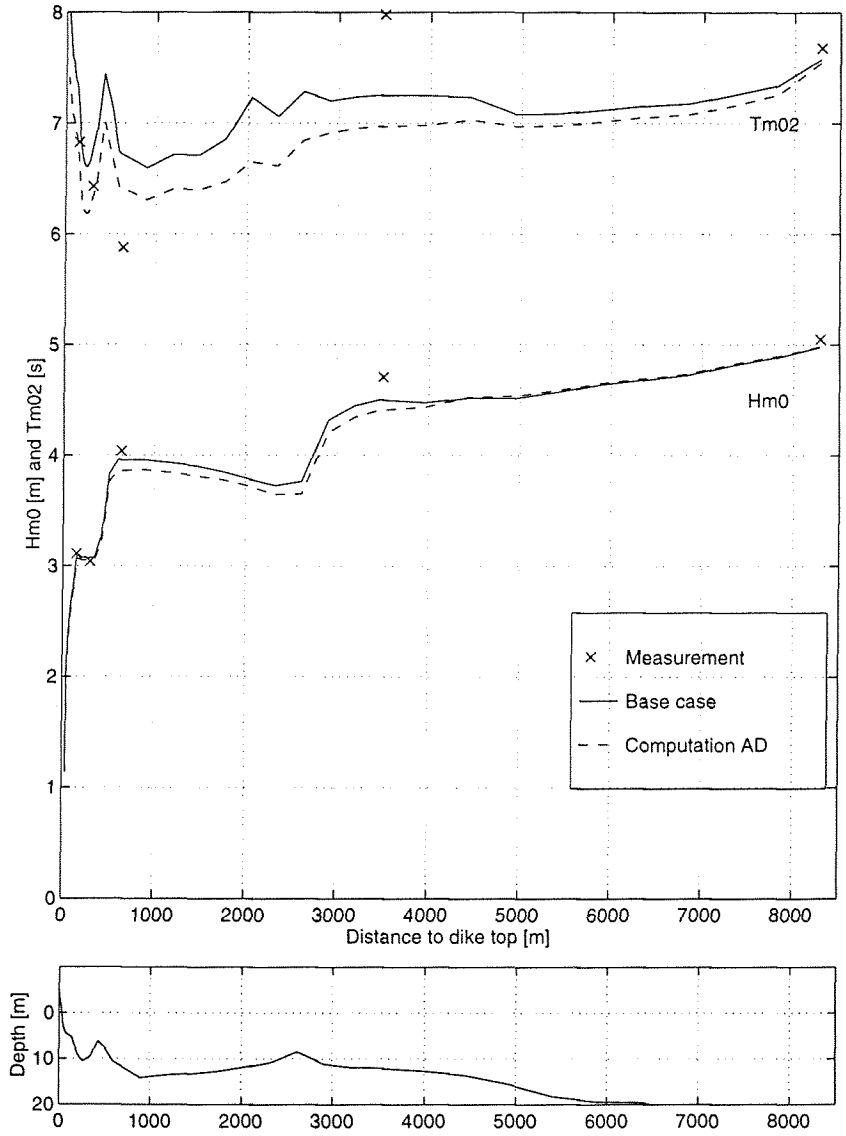

figure 5-14 Hm_0 and Tm_{02} along the Petten transect for case Ad

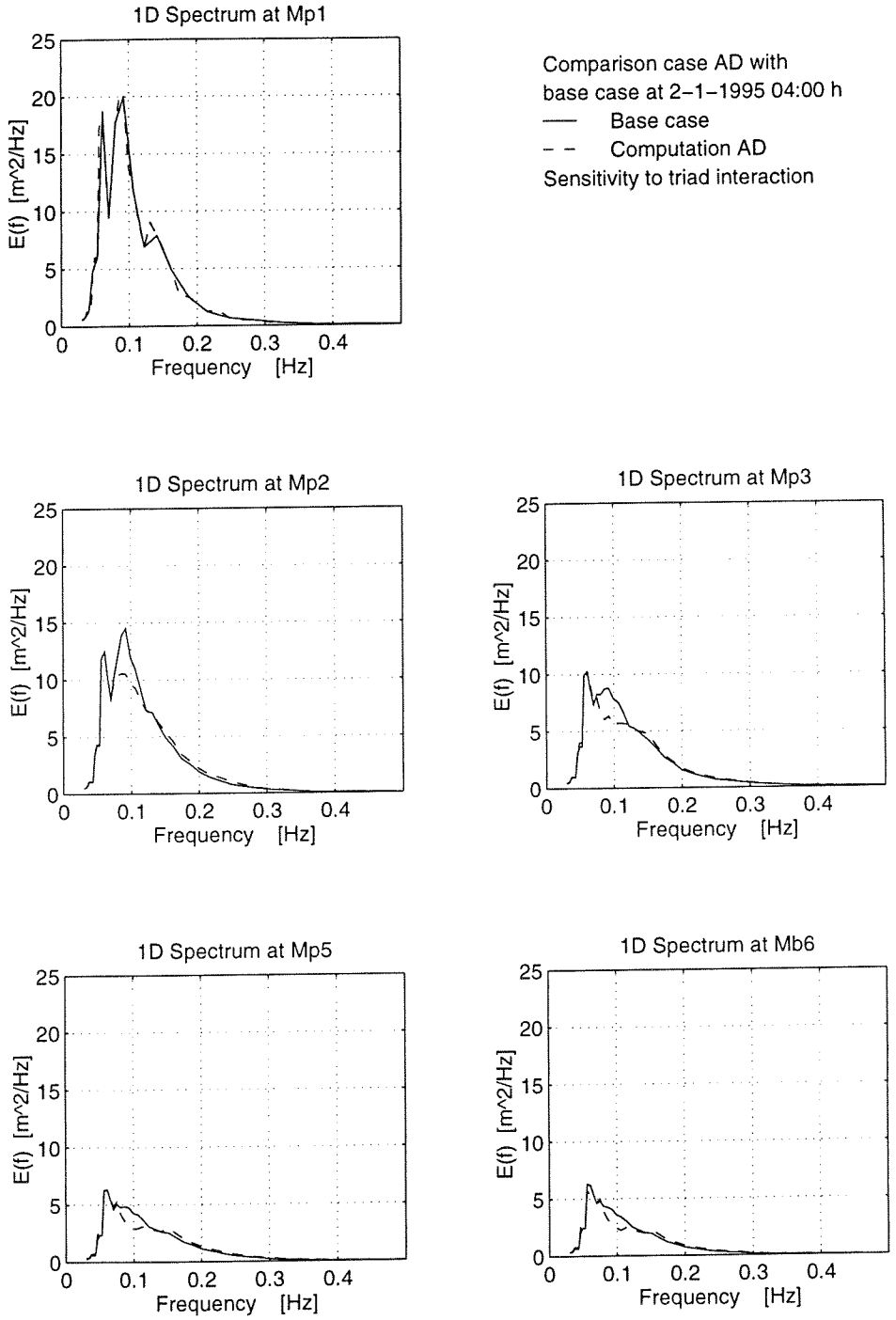

figure 5-15 Spectra along Petten transect for case Ad

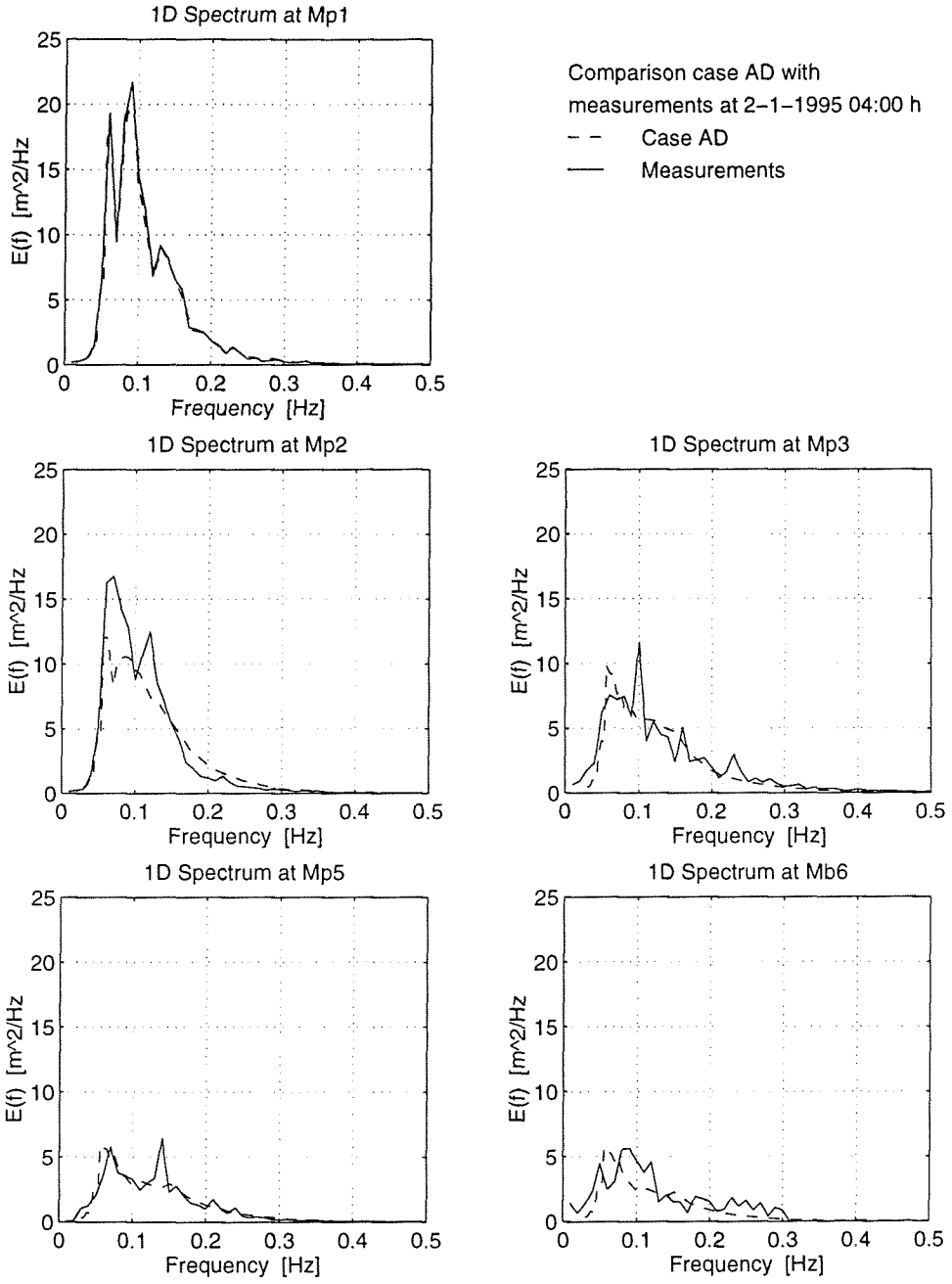

figure 5-16 Spectra along Petten transect for case Ad

A9 SWAN run in 2nd generation mode.

SWAN run in the second generation mode does not explicitly accounts for whitecapping but this is simulated in the wind input formulation.

The energy in this case is higher than for the base case. From 8300 m till 3500 m offshore far less energy is dissipated better match to measurements. At both breaker banks situated 3500 m and 600 m offshore more energy (than in the base case) is dissipated. The results nearshore (600 m and closer) are slightly better (closer to the observed waveheights) in 3rd generation mode than in 2nd generation mode.

For station Mp2 case A9 results in a better Hm_0 and Tm_{02} accordance with the observed values.

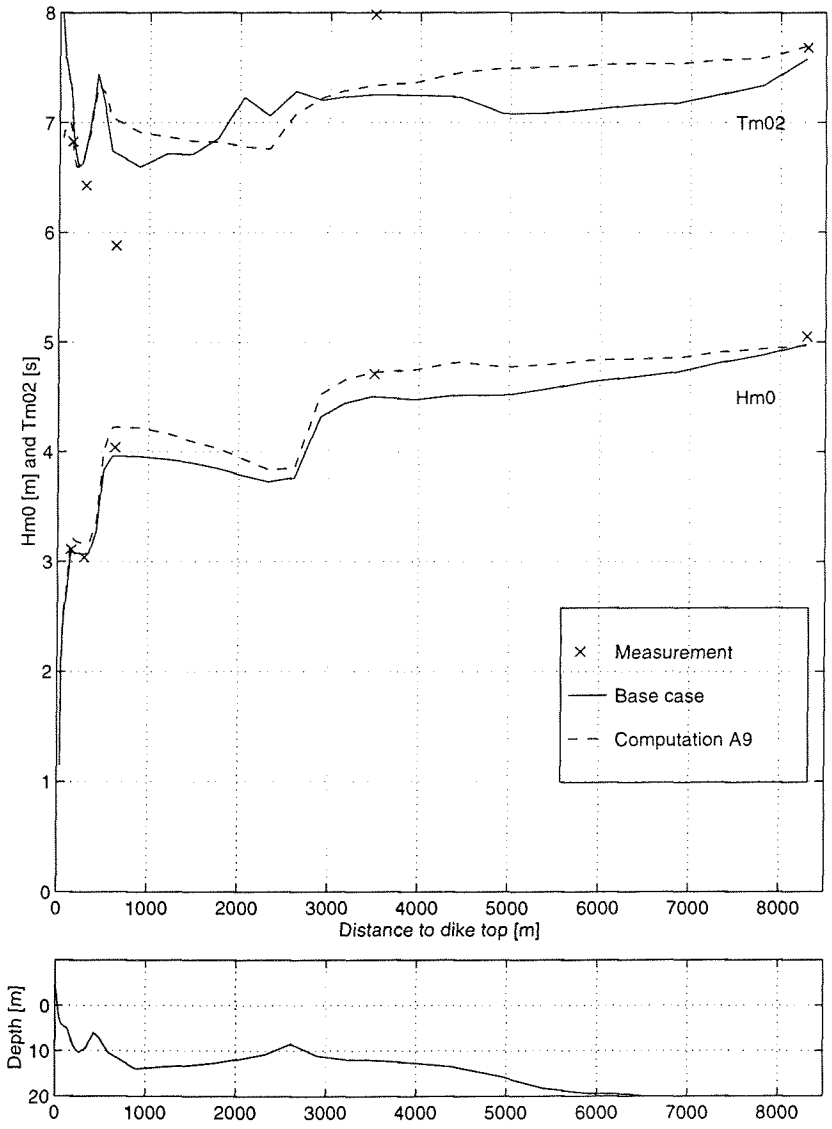

figure 5-17 **Hm_0 and Tm_{02} along the Petten transect for case A9**

Ac **Run with Janssen wind input instead of Komen wind input formulation.**

The wind input formulation by Janssen produces a smaller significant wave height than the formulation model by Komen (figure 5-18). The mean period Tm02 calculated with the Janssen is longer than the one calculated with Komen (base case). The results for Hm_0 calculated with Komen match the values of the observed waveheights better than the results computed with the Janssen schematization.

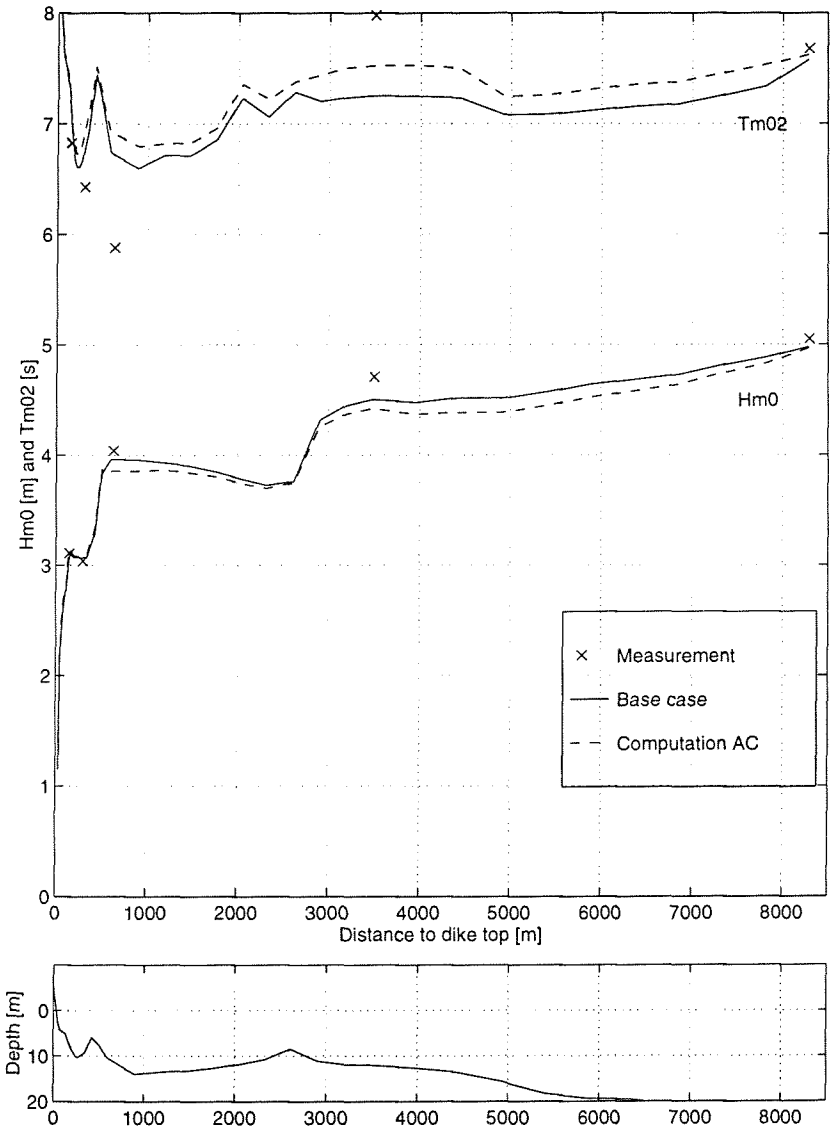

figure 5-18 **Hm_0 and Tm_{02} along the Petten transect for case AC**

6 Comparison between SWAN and HISWA

In this chapter the results from the SWAN computations are compared to HISWA computations for the same cases.

6.1 General

HISWA is the predecessor of SWAN. HISWA is, like SWAN, based on the action balance equation but it is not a fully spectral model. In HISWA the spectrum is discrete spectral only in the directions and parametric (contrary to SWAN) in the frequencies. A description of HISWA is given in section 2.2.3.

6.2 HISWA base case

Due to the numerical procedure in HISWA special attention needs to go to the size of the grid in x-y space. Also special attention needs to go to the orientation of the grid (so that the orientation of the x-axis is chosen to be about equal to the incoming mean wave direction).

HISWA computation	Fine model	Super fine model
Area Name:	area 2 HISWA.	Area 3 HISWA.
Origin: (Paris Coor.) [m]	94350. 530000	104500. 530800
Size: [m]	9000 X 16000	1000 X 2000
Rotation: [°] [clockwise]	35.	20.
Resolution: [Δx x Δy] [m]	75 x 107	8.3 x 20
Resolution: [meshes]	120 X 150	120 X 100
$\Delta\theta$: [°]	9	9

table 6-1 Orientation and size of grids of HISWA

The boundary conditions for the three cases to be modeled in HISWA are given in table 3-2.

The standard settings for all three cases are given in table 6-2.

Depth-induced breaking	$\gamma = 0.73$
Bottom friction	cfw = 0.01 cfc =0.005
Frequency change due to bottom friction	bf=0.5 (1)
Frequency change due to surf dissipation	bf=0.5 (1)

table 6-2 Standard settings HISWA

(1) bf=-1/(1-n) $E = C*k^{-n}$

Because of the conditions, the calculations in HISWA are done with the frequency shift for both depth-induced breaking and bottom friction switched on.

6.3 Comparison HISWA - SWAN

Case 1: 1-1-1995 16:00 h (U.T.C.)

figure 6-1 shows the significant wave height calculated for case 1 by SWAN and by HISWA. It can be seen that the wave height calculated with SWAN in this case decreases less rapidly than the wave height calculated in HISWA. The physical processes that influence the wave heights (and other spectral wave parameters for that matter) are modeled more fundamentally in SWAN. The performance indicator for Hm_0 for this SWAN computation is 0.83 while HISWA's is 0.78. All indices are given in table 6-3.

The mean period in HISWA show a decrease reflecting the bottom topography. It is possible to switch the frequency change off so this change does not occur. The mean wave frequency in HISWA is affected by bottom friction assuming that the wave energy dissipation takes place at the low frequencies only, so less energy is assumed in the low frequencies hence a higher mean frequency and a lower period nearshore (figure 6-1).

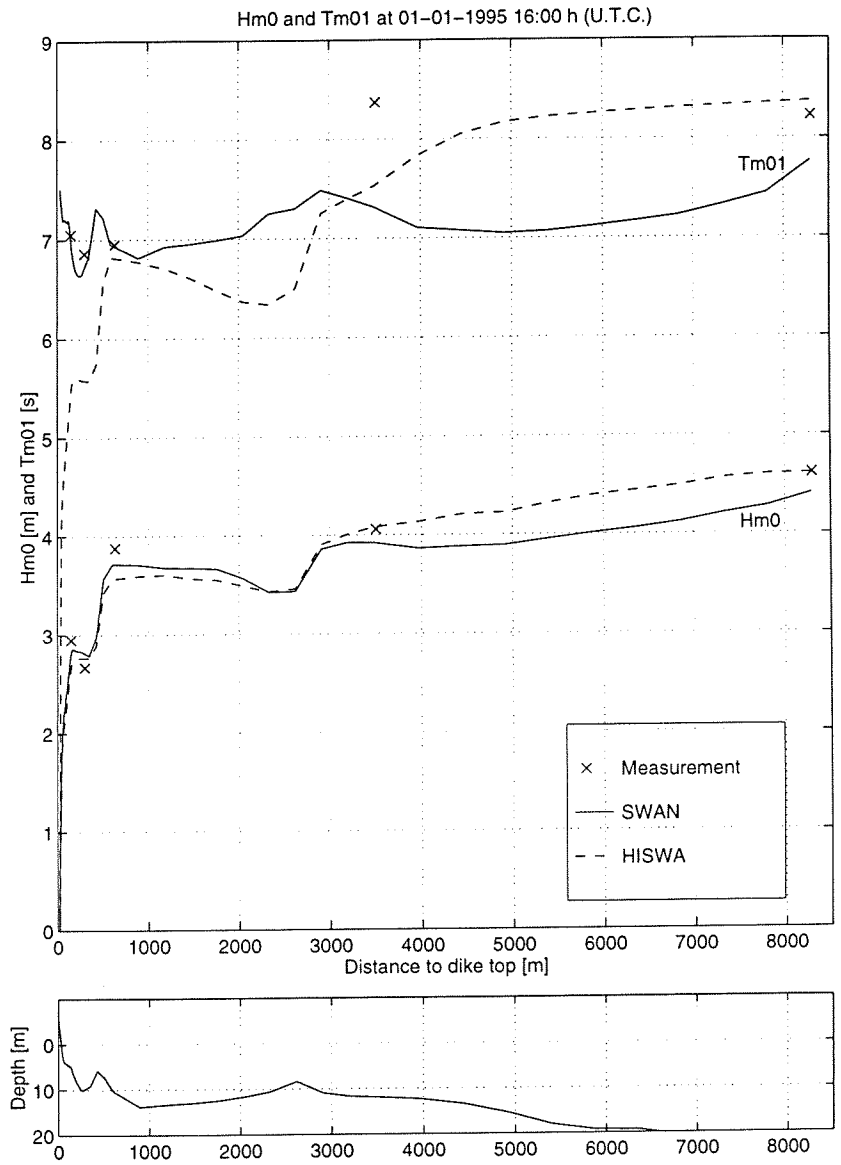

figure 6-1 **Hm_0 and Tm_{01} along Petten transect at 1-1-1995 16:00 h. (Comparison SWAN - HISWA)**

	SWAN	HISWA
Performance index	0.83	0.78
Scatter index	0.06	0.09
Boundary index	0.05	0.07

table 6-3 **Indices at 1-1-1995 16:00 h. (Comparison SWAN - HISWA)**

Case 2: 2-1-1995 04:00 (U.T.C.)

The performance indicator for Hm_0 in case 2 (figure 6-2) for the HISWA calculation is 0.71 The one for the SWAN calculation of the wave height is 0.87. All indices for this case are given in table 6-4. The performance of SWAN is better than the performance of HISWA. In HISWA the dissipation of energy is greater than that of SWAN.

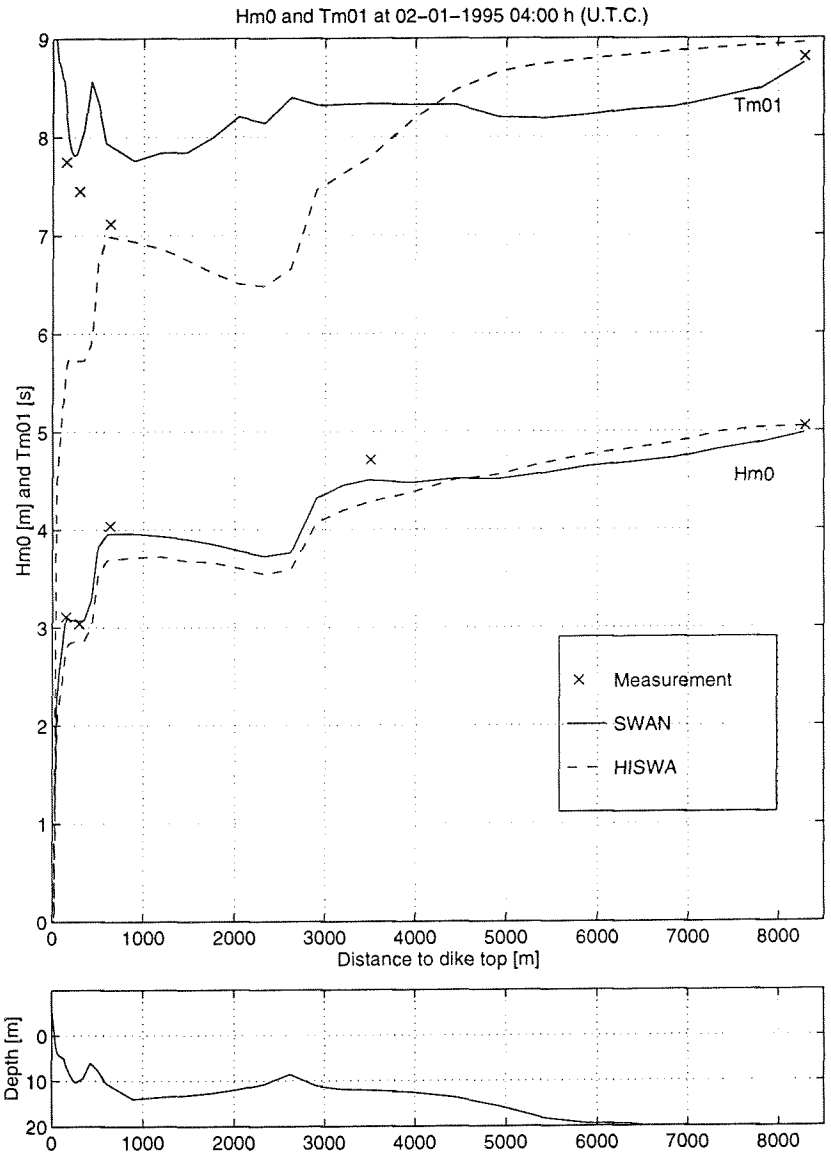

figure 6-2 **Hm_0 and Tm_{01} along Petten transect at 2-1-1995 04:00 h. (Comparison SWAN - HISWA)**

	SWAN	HISWA
Performance index	0.87	0.71
Scatter index	0.05	0.10
Boundary index	0.04	0.09

table 6-4 **Indices at 2-1-1995 04:00 h. (Comparison SWAN - HISWA)**

Case 3: 10-1-1995 11:00 h. (U.T.C.)

In this case (figure 6-3) the performance indicator for Hm_0 for the HISWA calculation is 0.75. for the SWAN computation it is 0.84. All indices are given in table 6-5.

Also in this case SWAN gives a better prediction than HISWA for both waveheights and periods.

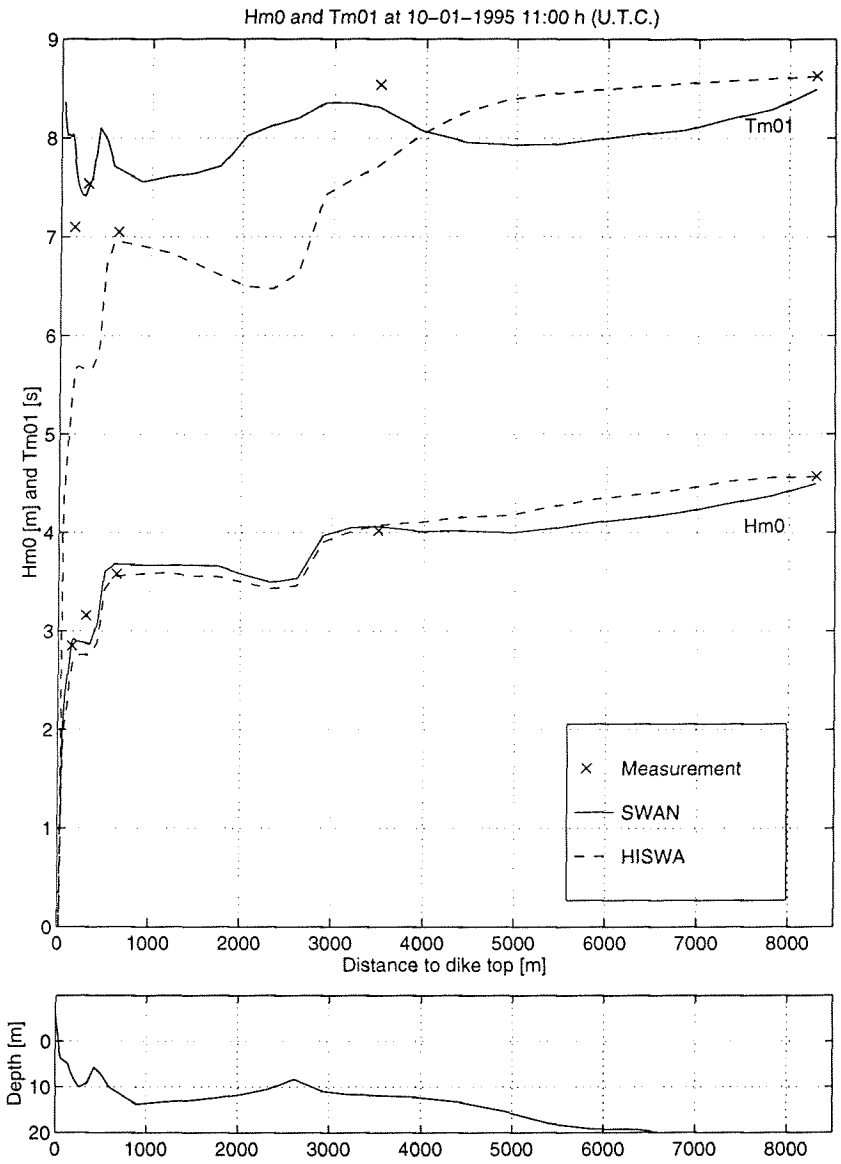

figure 6-3 **Hm_0 and Tm_{01} along Petten transect at 10-1-1995 11:00 h. (Comparison SWAN - HISWA)**

	SWAN	HISWA
Performance index	0.84	0.75
Scatter index	0.06	0.09
Boundary index	0.04	0.07

table 6-5 **Indices at 10-1-1995 11:00 h. (Comparison SWAN - HISWA)**

Case 2: 2-1-1995 04:00 (U.T.C.)

The frequency change is turned off for both bottom dissipation and surf dissipation in this case (figure 6-4). Energy redistribution due to nonlinear wave interactions is not taken in account in the HISWA computations. Energy redistribution is expected however. The indices for this case are presented in table 6-6.

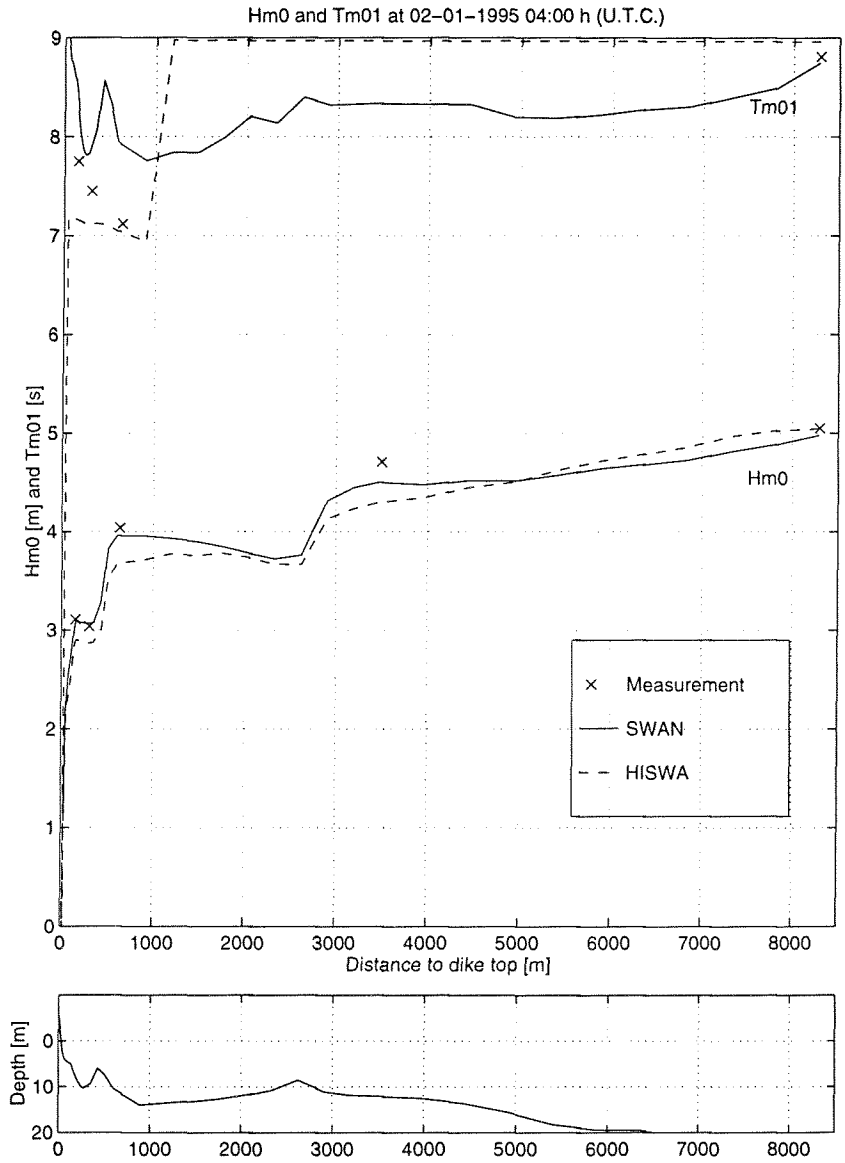

figure 6-4 **Hm_0 and Tm_{01} along Petten transect at 2-1-1995 04:00 h. (Comparison SWAN - HISWA) with frequency change off**

	SWAN	HISWA
Performance index	0.87	0.71
Scatter index	0.05	0.10
Boundary index	0.04	0.09

table 6-6 **Indices at 2-1-1995 04:00 h. (Comparison SWAN - HISWA)**

6.4 Performance HISWA - SWAN

For all cases all indices for SWAN computations are better than the same indices in HISWA.

The decrease in energy along the transect is for all cases bigger in HISWA, so that near the coast SWAN computations calculate higher values for Hm_0 than HISWA does. The variation of periods along the Petten transect differs considerably between HISWA and SWAN. This is because of the way the mean period is calculated in the models. The mean frequency is calculated from the energy distribution. This is calculated more fundamentally in SWAN (a 'parametrized' distribution over the frequencies not present in HISWA in which the energy distribution is parametrized by the zeroth and first order momentum only). SWAN is able to model nonlinear wave interactions. These nonlinear interactions redistribute energy over the frequencies so energy is able to shift not only between directional bins (like in HISWA) but also between frequency bins.

7 Conclusions and recommendations

7.1 Conclusions

The answer to the main question in this report, 'How do SWAN HISWA perform at the Petten coastal area' is GOOD. SWAN is able to give estimates for the Petten coastal area that are within accuracy of the devices used (within 6% error for Hm_0). So SWAN calculates good values for the energy density spectra as well as for the wave parameters for all stations.

HISWA also produces good estimates for wave heights (within 10%), but the estimates for mean wave periods in HISWA are not as good as in SWAN. SWAN gives better estimates than HISWA does for all cases studied.

SWAN computations starting at 20 km offshore Petten give estimates for the boundary conditions in station Mp1 (8.3 km offshore) that are within 10% for the wave heights and within 13 % of the periods (Tm_{01} and Tm_{02}) observed at this station Mp1.

The differences in spectral shape between approach 1 (starting at stations 20 km offshore) and approach 2 (starting at Mp1 8.3 km offshore) are small (see total energy and distribution (Hm_0 and periods)). The spectral shape calculated with approach 1 cannot reproduce exactly the shape measured at station Mp1 (8300 m offshore) because the exact shape of offshore spectrum for approach 1 is not known.

The spectral shape in approach 2 (computations starting at measuring point Mp1 8.3 km offshore) resembles the observed spectra well for all stations.

The calculated parameters in SWAN for the station nearest the coast differ most from the observations.

The local conditions of the bottom topography are dominant in the cases studied.

To compare periods of observed spectra with periods of calculated spectra it is essential to calculate the periods from the spectra over the same frequency range. Especially mean zero crossing periods (Tm_{02}) are very sensitive to energy in high frequencies.

7.2 Recommendations

The SWAN computations starting at the permanent measuring stations (ELD and YMW) at great distance from the coast produces good estimates for station Mp1 (8.3 km offshore) under storm conditions. So the outer model can be used to supply boundary conditions for the inner model in these conditions.

Further investigation is necessary to investigate model performance for extreme storm conditions.

Wave set-up is not accounted for in these computations. The wave set-up should be calculated in another model and input in SWAN as a water elevation field.

SWAN should have the possibility to input several spectra on one boundary so that a variation in wave spectra on the boundary is possible.

List of References

Andorka Gal J.H. ,(1996), Verification set Petten

Battjes, J.A. and Janssen P.A.E.M., (1978), Energy loss and set-up due to breaking of waves, Proc 16th Int. Conf. Coastal eng., Hamburg, 569-587

Battjes, J.A., (1986), Lecture notes Windwaves, (D.U.T.) (in Dutch)

Booij, N. and Holthuijsen, L.H., (1995) HISWA user manual

Cavaleri,L. and Malanotte-Rizzoli,p. (1981), Wind wave prediction in shallow water: Theory and applications. J. Geophys. Res 86, No C11, 10, 961-10, 973

Dekker,J., Hartsuiker,G. (1995), Extreme wave conditions along the coast of the Netherlands.

Dunsbergen, D.W. (1995) Validation of SWAN 20.51 against field measurements in the Friesche Zeegat

Holthuijsen,L.H., Booij,N. and Herbers,T.H.C. ,(1989) , A prediction model for stationary, shortcrested waves in shallow water with ambient currents. Coastal Engineering, 13, 23-54

Holthuisen,.L.H., Booij,N. and Ris,.R.C., (1993), A spectral wave model for the coastal zone.

Holthuijsen,L.H., Eldeberky,Y., Booij,N. Ferier,P. (1994), The maximum significant wave height in the southern North Sea.

Komen,G.J., Cavaleri,L., Donelan,M. Hasselmann,K., Hasselmann,S. and Janssen,P.A.E.M., (1994), Dynamics and Modeling of Ocean Waves, Cambridge University Press

Otta,A.K., van Vledder,.G.Ph., Holthuijsen,L.H., and Ris,R.C., (1995), Validation of SWAN against field and experimental data

Ris,R.C., Booij,N. and Holthuijsen,L.H., (1996), SWAN Cycle 1 user manual

Ronde,J.G. de, Marle,J.G.A.., Roskam.A.P., Andorka Gal,J.H., (1995), Golfrandvoorwaarden langs de Nederlandse kust op relatief diep water, (in Dutch).

Roskam,A.P., Hoekema,J., (1995), Verwerking van Egmond 1982 meting EG2320 ten behoeve van: de validatie van golfmodellen in zeer ondiep water, de bepaling van golfparameters in zeer ondiep water, (in Dutch).

Ruessink,B.G., (1995), Calculation of wave heights from pressure time series.